Project Report
ATC-395

Multifunction Phased Array Radar (MPAR) Spectral Usage Analysis

J.Y.N. Cho
S.M. Duffy
R.D. Grappel

24 July 2012

Lincoln Laboratory
MASSACHUSETTS INSTITUTE OF TECHNOLOGY
LEXINGTON, MASSACHUSETTS

Prepared for the Federal Aviation Administration,
Washington, D.C. 20591

TECHNICAL REPORT STANDARD TITLE PAGE

1. Report No.	2. Government Accession No.	3. Recipient's Catalog No.
ATC-395		

4. Title and Subtitle	5. Report Date
Multifunction Phased Array Radar (MPAR) Spectral Usage Analysis	24 July 2012
	6. Performing Organization Code

7. Author(s)	8. Performing Organization Report No.
John Y.N. Cho, Sean M. Duffy, and Robert D. Grappel	ATC-395

9. Performing Organization Name and Address	10. Work Unit No. (TRAIS)
MIT Lincoln Laboratory 244 Wood Street Lexington, MA 02420-9108	11. Contract or Grant No. FA8721-05-C-0002

12. Sponsoring Agency Name and Address	13. Type of Report and Period Covered
Department of Transportation Federal Aviation Administration 800 Independence Ave., S.W. Washington, DC 20591	Project Report
	14. Sponsoring Agency Code

15. Supplementary Notes

This report is based on studies performed at Lincoln Laboratory, a federally funded research and development center operated by Massachusetts Institute of Technology, under Air Force Contract FA8721-05-C-0002.

16. Abstract

This report addresses two technical risks associated with replacing current air traffic and weather surveillance radars with a single type of multifunction phased array radar (MPAR). The first risk is whether radio spectrum usage would increase with the MPAR network and whether the allocated band will have enough spectral space. This question is addressed in two steps. First, single-radar spectrum usage is estimated based on certain assumptions regarding the radar design. Second, locations based on a previous radar placement study are used together with a terrain-dependent propagation model to compute the number of frequency channels needed at each site. We conclude that the overall spectrum usage is likely to increase with MPAR, but that the targeted window in S band will be able to accommodate the occupancy at all sites.

The second risk is whether self-interference will limit the ability of the MPAR to operate asynchronously and adaptively on different antenna faces. This question is addressed by employing a simple bistatic ground clutter model to characterize the interference between adjacent faces. We conclude that some interference is unavoidable, but it would likely only occur during times when a transmit beam is at its maximum off-broadside angle (~2% of the time).

17. Key Words	18. Distribution Statement
	This document is available to the public through the National Technical Information Service, Springfield, VA 22161.

19. Security Classif. (of this report)	20. Security Classif. (of this page)	21. No. of Pages	22. Price
Unclassified	Unclassified	72	

FORM DOT F 1700.7 (8-72) Reproduction of completed page authorized

This page intentionally left blank.

EXECUTIVE SUMMARY

The multifunction phased array radar (MPAR) is a candidate solution to the Federal Aviation Administration's (FAA) Next Generation Air Transportation System (NextGen) Surveillance and Weather Radar Capability (NSWRC). As a concept under development, it has areas of technical risk that need to be explored and mitigated if possible. One such risk area is radio frequency (RF) spectral usage. Unlike traditional single-use ground-based radars that are used for civil-sector weather and aircraft surveillance, MPAR, by definition, will need to fulfill multiple missions at the same time. The RF spectral space is a degree of freedom that most likely will need to be exploited in order to meet all the observational objectives. This report describes the findings of a preliminary look into this topic.

The risk manifests itself in two areas. First, if spectral occupancy per radar is, indeed, increased relative to the legacy radars, will the radars be able to operate without undue interference within the allocated band? Second, could self-interference limit the ability of the MPAR to fully exploit the spectral frequency space for accomplishing its missions?

We tackled these questions by assuming a particular configuration for the MPAR, namely that it will have four antenna faces, and that there will be a full-size (8-m diameter antenna) version and a scaled down (4-m diameter antenna) version for terminal use (TMPAR). We also assumed that the new radars will be required to conform to the existing Radar Spectrum Engineering Criteria (RSEC), Group D, which applies to the 2.7–2.9 GHz band.

To study the first question, we estimated the single-radar spectral usage for the following operational cases: (A) all antenna faces operating at the same frequencies, (B) the front and back faces operating at the same frequencies, and (C) all faces operating on different frequencies. We also allowed each antenna face to have up to three parallel operational frequencies. The geographic locations of the MPARs and TMPARs were taken from a siting analysis detailed in a separate report. Three legacy radar replacement scenarios were examined: (1) only the terminal aircraft and weather radars are replaced, (2) in addition to the Scenario 1 radars, NEXRADs are replaced, and (3) in addition to the Scenario 2 radars, en route aircraft surveillance radars are replaced. For all operational cases and replacement scenarios, co-channel interference between radar pairs were computed based on the single-radar results and a terrain-dependent RF propagation model. The analysis showed that there would be sufficient space in the targeted spectral window (2.7–2.9 GHz for Scenario 1, 2.7–3.0 GHz for Scenarios 2 and 3) for all cases considered. There is a caveat, however, in that the transition period when both the legacy and the new radars are operating at the same time was not studied. (Also, tactical military air surveillance radars were not included.) Therefore, a more detailed site-by-site spectral allocation analysis should eventually be conducted in conjunction with an MPAR deployment plan that specifies the exact locations of the new (or temporary) radars during the transition period.

To analyze the second question, we employed a simple bistatic ground clutter model to characterize the interference between adjacent antenna faces. (Too much interference between faces would disallow independent, asynchronous operation of the four antennas, which, in turn, would severely restrict adaptive

operation that is a key attractive element of MPAR. In other words, operation would be restricted to Case A above.) The results showed that some interference is unavoidable, but it would likely only occur during times when a transmit beam was at its maximum off-broadside angle of 45° (~2% of the time). The consequent degradation in data quality due to "dead" gates in the adjacent-face receiver could be compensated for by adaptively increasing the dwell on receive. A caveat of this part of our study is that important effects such as diffraction from the radome and face edge, tower structure, and mutual coupling were not included. We recommend a follow-on study that employs a more detailed electromagnetic model that can exposes the risks in fuller measure, which could also be used to explore other mitigation strategies.

TABLE OF CONTENTS

This page intentionally left blank.

LIST OF ILLUSTRATIONS

LIST OF ILLUSTRATIONS
(Continued)

LIST OF ILLUSTRATIONS
(Continued)

This page intentionally left blank.

LIST OF TABLES

This page intentionally left blank.

1. INTRODUCTION

The workhorse sensor for aircraft and weather surveillance today in the U.S. is the ground-based radar. Several different radar types operating at various frequency bands are used for specific missions (Figure 1-1). As the radar systems inevitably age, they need to be maintained and upgraded through service life extension programs or replaced. One proposed alternative to maintaining or replacing each radar type separately is the deployment of a network of multifunction phased array radars (MPARs) that would supersede some or all of these legacy radars (Benner et al., 2009). MPARs would operate in the band currently occupied by the Airport Surveillance Radars (ASRs) and Next Generation Weather Radar (NEXRAD) (Figure 1-2), and be able to accomplish all of the missions conducted by the current multiplicity of radars with just one type of radar. The Federal Aviation Administration (FAA) is currently considering the MPAR as a possible solution to its Next Generation Air Transportation System (NextGen) Surveillance and Weather Radar Capability (NSWRC).

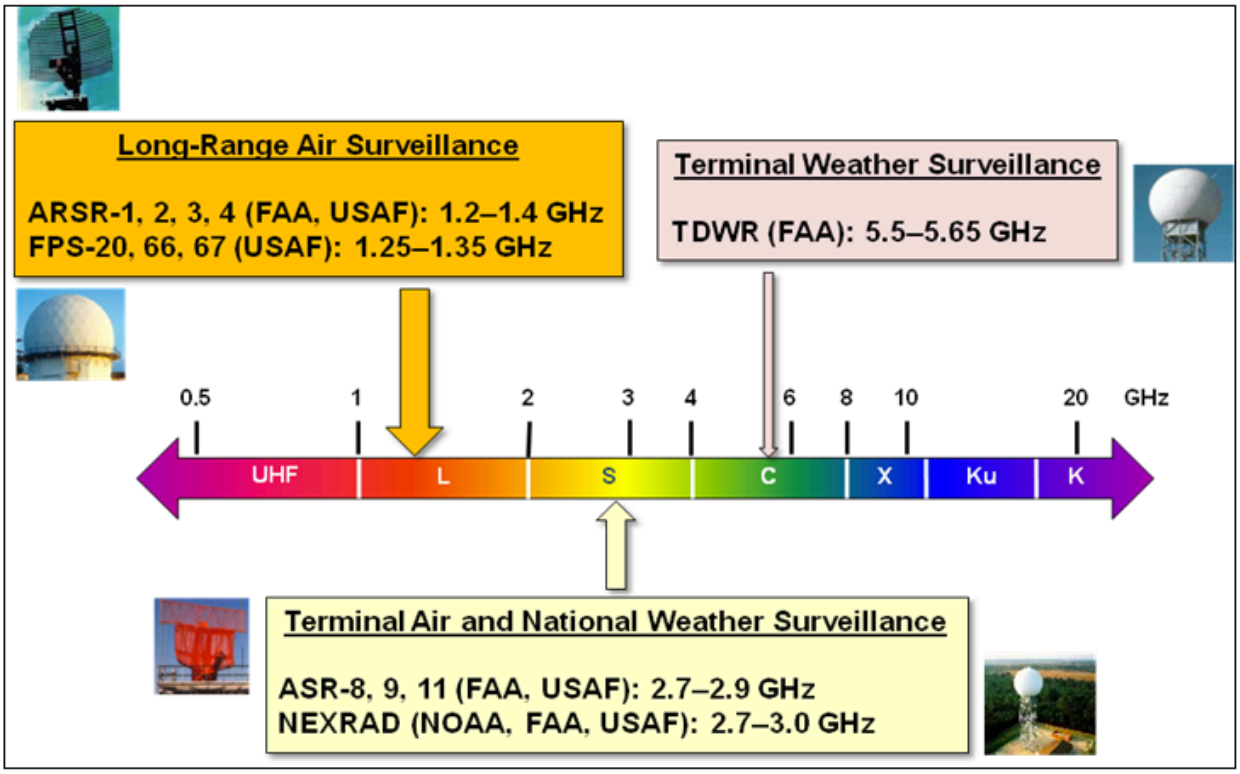

Figure 1-1. Operational frequency bands of the current U.S. aircraft and weather surveillance radars that may potentially be replaced by MPAR.

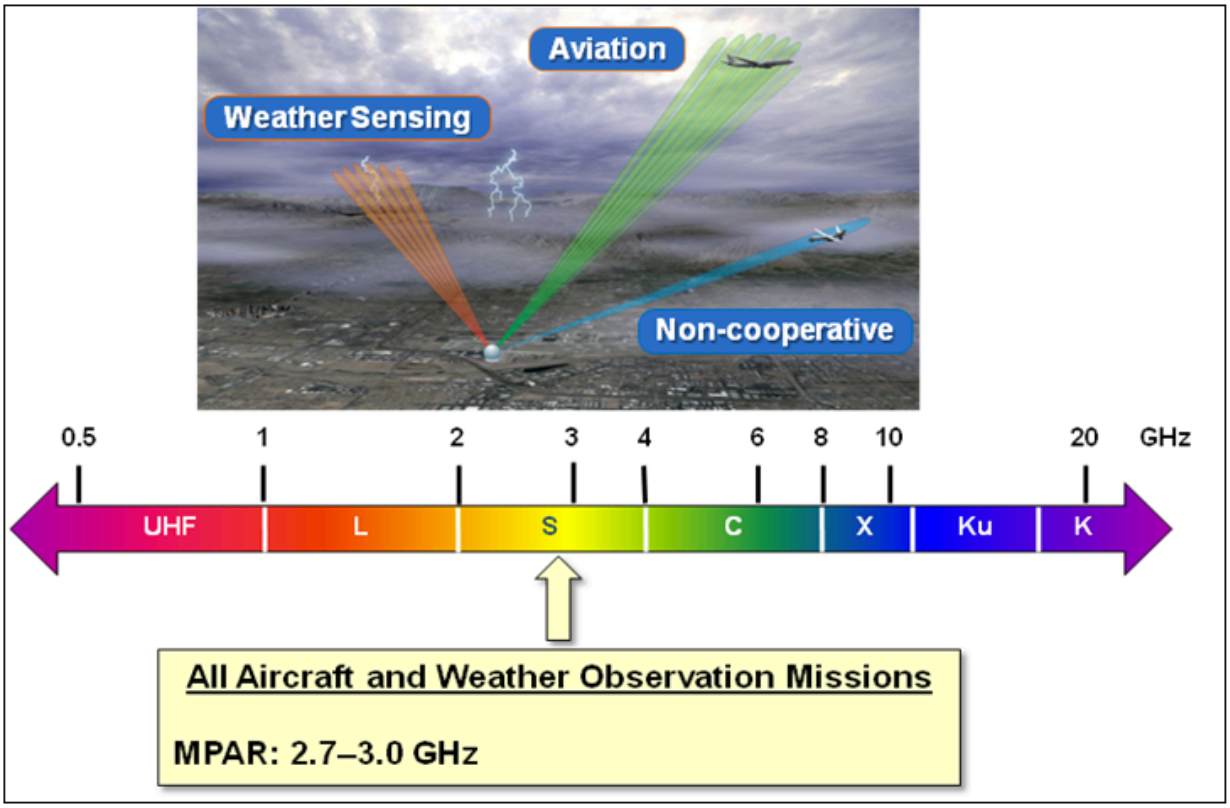

Figure 1-2. Operational frequency band of the proposed MPAR network.

The legacy radars broadcast in Federal government-owned spectral bands that are off limits to commercial operators. (The exception is the Terminal Doppler Weather Radar's (TDWR) operating band, which was opened up to sharing with unlicensed national information infrastructure (U-NII) devices in 2003 (FCC, 2003).) With the rapid expansion of the broadband wireless market in recent years, there has been increasing pressure to free up more government spectral windows for commercial use. A 2010 White House memo decreed that 500 MHz of radio frequency (RF) spectrum be made available for mobile and fixed wireless broadband use in ten years (Obama, 2010). On one hand, the MPAR program promotes more efficient use of the frequency spectrum by consolidating the current surveillance missions conducted in different frequency windows into one band. On the other hand, the deployment of the MPAR network may increase spectral usage in the 2.7–2.9 GHz band, which is one of the windows targeted by the National Telecommunications and Information Administration (NTIA) for opening up to sharing with the wireless broadband community. Because MPAR must conduct multiple surveillance missions, the RF spectral domain is an important degree of freedom that needs to be exploited in order to

meet the update requirements for all missions. Thus, it is crucial to quantify how much spectral space will be required by the MPAR network.

We studied this issue in two parts. First, we estimated the spectral usage of a single MPAR system. Then, given the single-radar usage and the locations of the radars as determined by our siting analysis, we ran a frequency assignment algorithm to determine how much spectral occupancy could be expected for the entire network. We also analyzed the potential interference between the different antenna faces of a single MPAR and its operational implication.

This page intentionally left blank.

2. SINGLE RADAR SPECTRAL USAGE

The RF spectral usage of an active phased array radar differs fundamentally from a mechanically scanned dish antenna radar in two ways. (1) A phased array radar usually has two or more separate antenna faces. If independent, asynchronous operation is desired for each face, then the faces need to be isolated from each other, which likely will lead to operation at different frequencies. (2) Unless high peak-power elements are employed (which makes a phased array extremely expensive), the lower peak-power capability (relative to a single-dish or passive phased array system) necessitates the use of long transmitted pulses (with compression coding) for long-range observation and short pulses for close-range observation (Figure 2-1). Frequency separation is normally employed to operationally isolate the two pulse types.

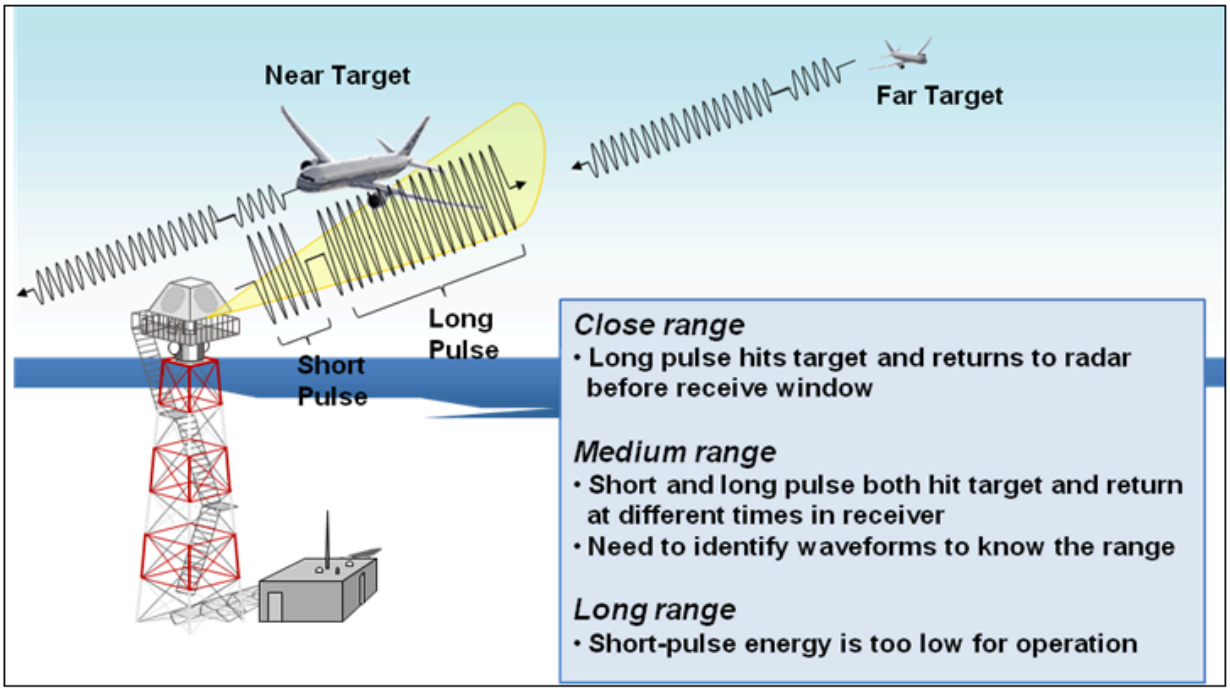

Figure 2-1. Illustration of simultaneous long and short range observation using a combination of long and short pulses.

The multiple mission aspect of MPAR may impose further demands on spectral usage. For example, if the update time requirements for all missions cannot be met with sequential scanning,

simultaneous scanning may need to be implemented using parallel frequency channels. Bandwidth will also depend on the mission requirements. For example, if MPAR is required to perform identification of air vehicle type (not currently foreseen as a requirement), then ultra-high bandwidth (~200 MHz) will be needed for very fine range resolution.

For the analysis to follow, we made these assumptions.

- There will be a full-sized MPAR (8-m diameter array per face) and a scaled down terminal MPAR (TMPAR, 4-m diameter array per face).
- There will be four antenna faces, arranged along a square-shaped perimeter, per radar.
- Each face will transmit a long (compression coded) pulse and a short (unmodulated) pulse. The two pulses will be separated in frequency.
- MPAR and TMPAR will only meet existing observation requirements for weather and aircraft surveillance (see Appendix A for a table of relevant legacy requirements for representative radars). Air vehicle identification requirements will not be imposed.
- The emission spectrum will meet the Radar Spectrum Engineering Criteria (RSEC), Group D (NTIA, 2011).

The RF spectrum of a transmitted pulse is dependent on the pulse power, length, shape, and waveform modulation. These parameters, in turn, are determined by the performance and interference mitigation requirements. The required radar peak powers have previously been determined and are given in Table 2-1. The values include losses up to the antenna radiator. (NEXRAD is included, because one of the MPAR deployment scenarios that the FAA is considering calls for only the terminal radars to be replaced, leaving the NEXRADs to share the same frequency band as the NSWRC radars.) The pulse length (1 μs) of the short-pulse mode is set by the legacy range resolution requirement of the TDWR (Appendix A). The maximum length of the long pulse is determined by the balance between sensitivity at long range and at the farthest end of the fill pulse (short pulse) mode; the actual lengths used may be shorter than that shown in Table 2-1, but we wish to be conservative for now. The NEXRAD also has a "long pulse" mode for clear-air observation, but it is unmodulated. We will only deal with the short pulse mode in this study as its much wider bandwidth represents the worse case for interference.

TABLE 2-1
Specified and Estimated Radar Parameters

Parameter		MPAR	TMPAR	NEXRAD
Peak power (dBm)		82	76	87
Antenna gain (dB)		46	41	45.5
Short pulse length (μs)		1	1	1.57
Max. long pulse length (μs)		730	40	N/A
Duty cycle (%)		0.2 (short), 24 (long)	0.2 (short), 7 (long)	0.2
–40 dB transmit bandwidth (MHz)	Short pulse	10.4	10.4	12.4
	Long pulse	3.8	3.8	N/A
–6 dB receiver filter bandwidth (MHz)	Short pulse	1.1	1.1	0.8
	Long pulse	1.4	1.4	N/A
Receiver noise density (dBm/MHz)		–110	–110	–111
Transmit noise floor (dB)		–111	–108	–110

All fixed radars in the 2.7–2.9 GHz band must meet RSEC emission spectrum Criteria D. For unmodulated pulse radars, the –40-dB bandwidth must be less than or equal to $6.2/(t_r t)^{1/2}$, where t_r is the rise/fall time and t is the pulse length, both in μs. We chose t_r = 0.2 μs with a sine taper for the short pulse, resulting in a theoretical –40-dB emission bandwidth of 10.4 MHz, which meets the RSEC limit. Beyond the –40-dB bandwidth, Criteria D specifies a decay of 40 to 80 dB per decade. We selected the latter limit to be strict, and generated a short-pulse composite emission spectrum using the theoretical results inside the 10.4-MHz bandwidth and the RSEC envelope outside (Figure 2-2). We did this because the actual spectral roll off will be likely less steep than the theoretical roll off. Finally, we imposed a transmit pulse noise floor relative to the peak as given in Table 2-1. The NEXRAD figure of –110 dB relative to the fundamental was estimated as a typical klystron value (Hinkle, 1983).

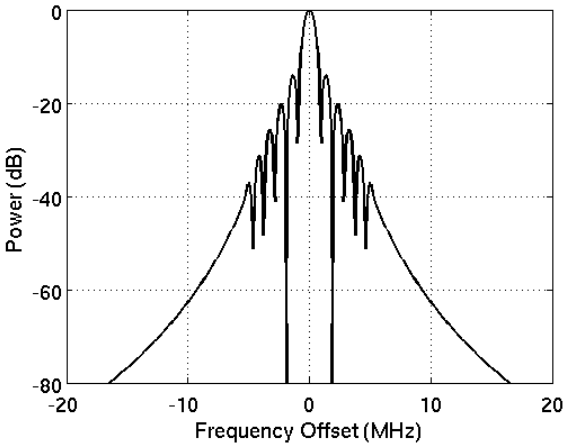

Figure 2-2. MPAR and TMPAR short pulse composite emission spectrum.

Setting parameters for the long pulse is a more complicated affair. In order to maintain the required range resolution, compression coding is necessary. However, at the same time, the range side lobes must be kept to a minimum. Because weather is generally a range-extended target with high dynamic range, the integrated side lobe level (ISL), not just the peak side lobe level, must be suppressed. Previous work has shown that nonlinear frequency modulation (FM) with tapering is a good choice to meet these goals. We opted to follow the weakly nonlinear scheme of O'Hora and Bech (2007), which adds amplitude tapers and slow-downs in frequency change at the pulse edges to a standard linear chirp (Figure 2-3). The total sweep in frequency is 3 MHz over the pulse length, with rise/fall time of 3 μs. The resulting transmit spectrum (again, composited with the RSEC mask beyond the –40-dB bandwidth) is shown in Figure 2-4.

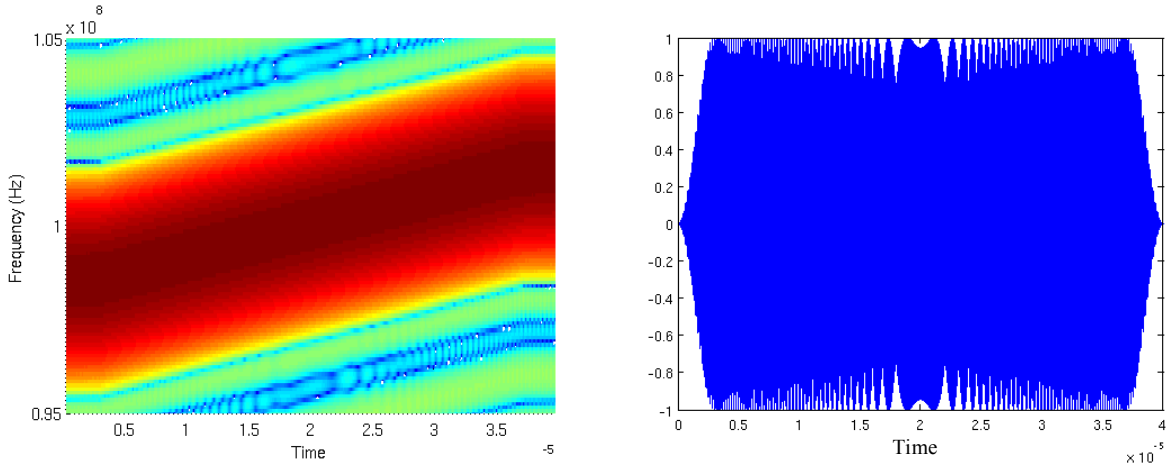

Figure 2-3. Spectrogram (left) and amplitude (right) vs. time plots of TMPAR long pulse waveform.

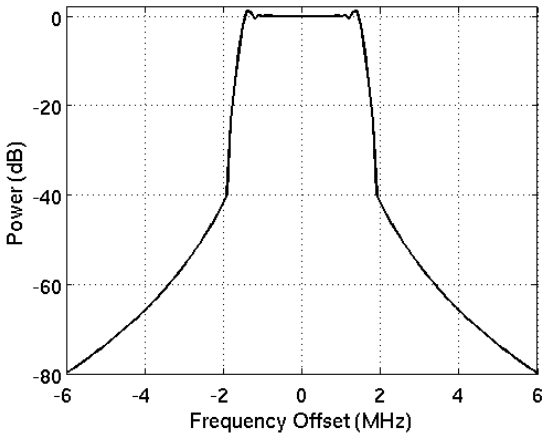

Figure 2-4. MPAR and TMPAR long pulse composite emission spectrum.

Combined with a mismatched spectral window, this scheme allows ISL of –40 dB for a $\cos^3$ window and –55 dB for a Blackman-Harris window, with corresponding gain losses of –1.7 dB and –3.5 dB, based on a simple trial-and-error process, while maintaining the required range resolution. A more systematic optimization will likely enable a better balance between ISL and gain loss, and more aggressively nonlinear FM waveforms could also be used if needed (e.g., George et al., 2010). Note, also, that amplitude shaping may be difficult as active phased array transmitters are usually operated in

saturation mode. However, selection of an optimal waveform is outside the scope of this study and there is no established requirement for ISL, so we will proceed with the pulse shown in Figure 2-3.

If two frequency channels (long and short pulse transmissions) are needed per antenna face in sequential scanning mode, how many in total are necessary for one MPAR? The answer depends on the choice of operational scenario. For example, if transmission from all faces were continuously synchronized to occur simultaneously, then frequency isolation between faces would likely not be necessary. In this case, however, each antenna face could not be operated independently and adaptively, a capability that is one of the strong selling points of an active phased array radar. Another option is to allow only the front and back faces to share the same frequencies; this would enable all faces to operate independently if the front-to-back isolation is good enough without frequency separation. Finally, one can assign different channels to each of the four faces. These scenarios are summarized in Table 2-2.

TABLE 2-2
MPAR Sequential Scanning Operational Scenarios

Scenario	Frequencies	Implications
All faces independent frequencies	8	Large spectral content at each site, most flexible
Front and back faces share frequencies	4	Front-to-back isolation is critical specification
All faces share frequencies	2	No adaptive operation allowed

The discussion so far has assumed that all of the required surveillance missions can be accomplished through sequential scanning. If, however, it is determined that the various observational missions cannot be fulfilled with this approach, it may become necessary to perform scans in parallel on different frequency channels. For example, the two frequencies used for the short- and long-pulse modes could be opened up for general parallel operation. If even that is not enough, then three independent channels could be set up for parallel transmission and reception. In this case, the total number of frequencies per radar would increase to 12 for the “all faces independent” case, six for the “front and back faces share frequencies” case, and three for the “all faces share frequencies” case. In the next section, all of these scenarios will be analyzed for multiple radar spectral usage.

3. MULTIPLE RADAR SPECTRAL OCCUPANCY

This section will describe the frequency allocation program that was developed to determine the number of frequencies that would be required to implement a set of three possible scenarios for the installation of MPAR and TMPAR systems to replace existing surveillance and weather radars in the U.S. and its territories. The three scenarios are (1) Terminal radars only (ASRs and TDWRs), (2) terminal radars and national-scale weather radars (ASRs, TDWRs, and NEXRADs), and (3) all radars (ASRs, TDWRs, NEXRADs, ARSRs, and Fixed Position Systems (FPSs)). Figures 3-1 to 3-3 show the proposed locations of the MPARs and TMPARs for each scenario (Cho et al., 2012). Figure 3-1 also shows NEXRAD locations, since they will still be in place for Scenario 1.

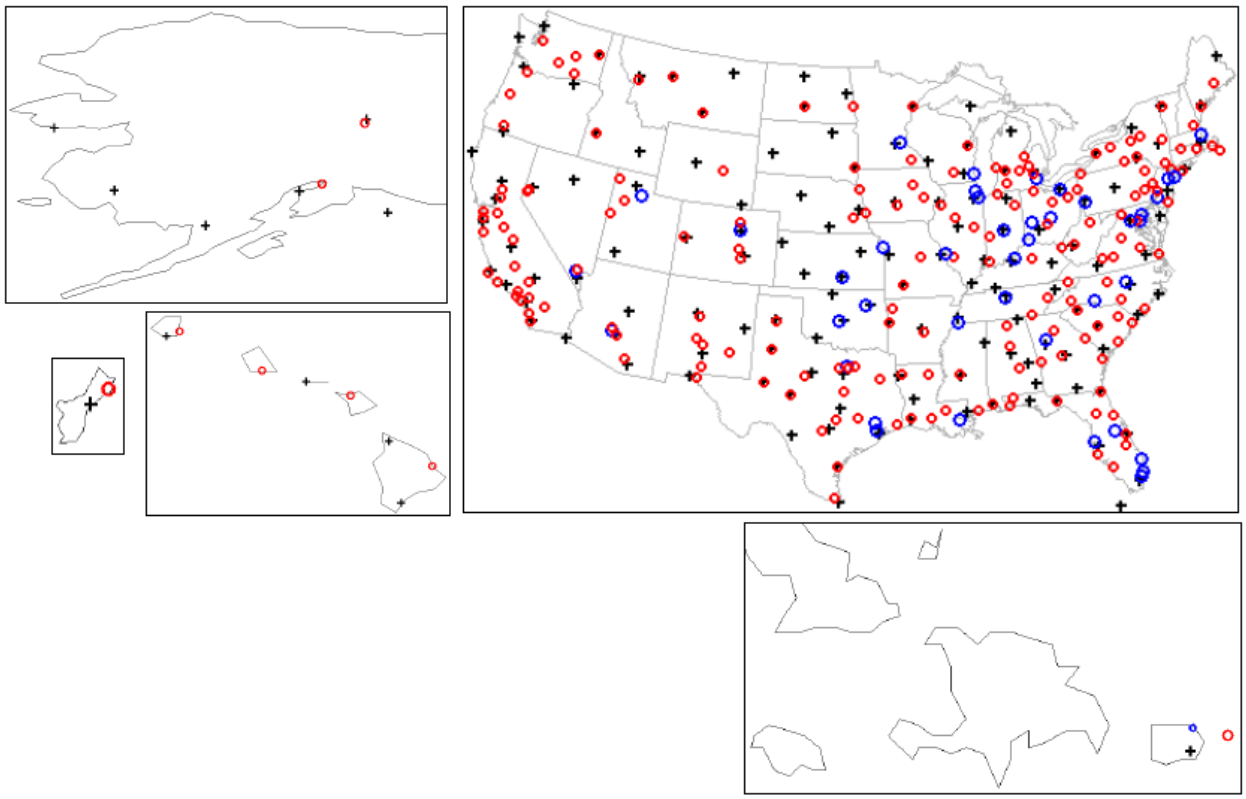

Figure 3-1. Locations of MPAR (blue circle), TMPAR (red circle), and NEXRAD (black cross) for Scenario 1. Clockwise from top left: Alaska, contiguous United States, Puerto Rico/Virgin Islands/Guantanamo Bay, Hawaii, and Guam.

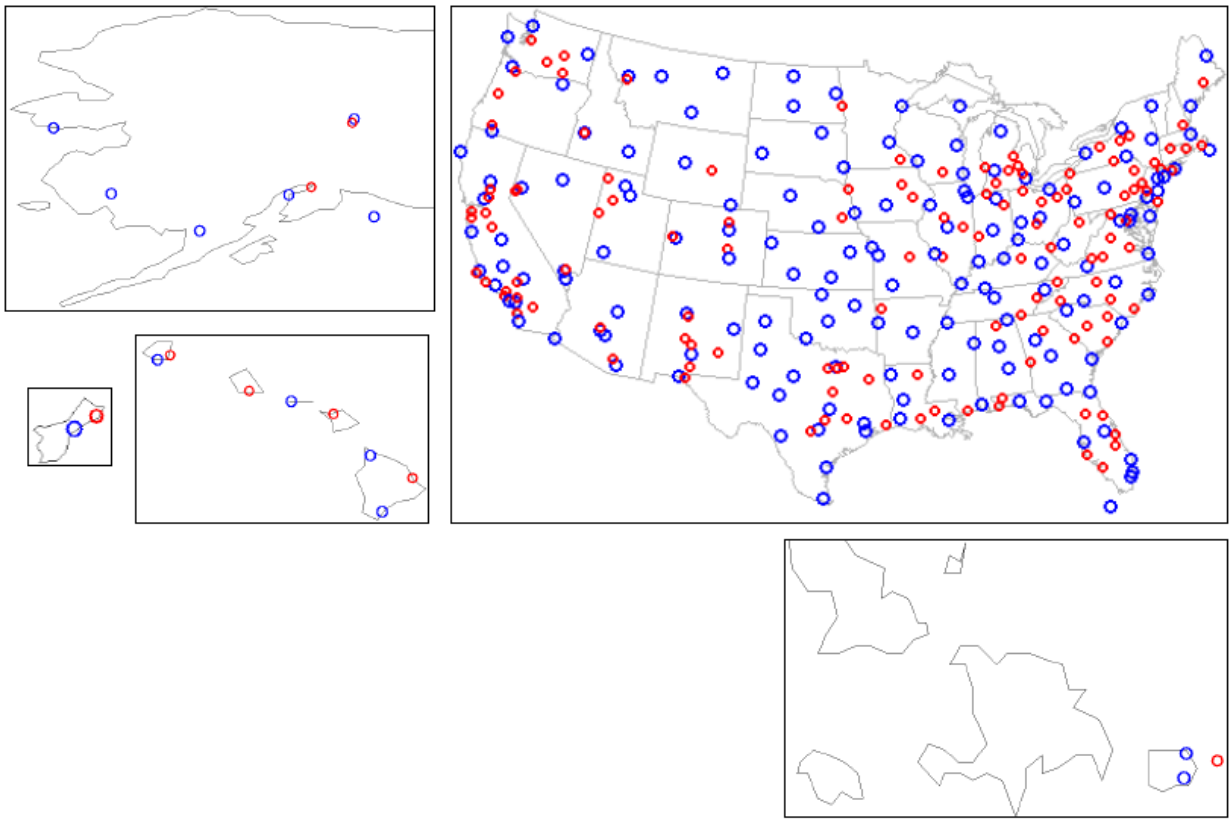

Figure 3-2. Locations of MPAR (blue) and TMPAR (red) for Scenario 2. Clockwise from top left: Alaska, contiguous United States, Puerto Rico/Virgin Islands/Guantanamo Bay, Hawaii, and Guam.

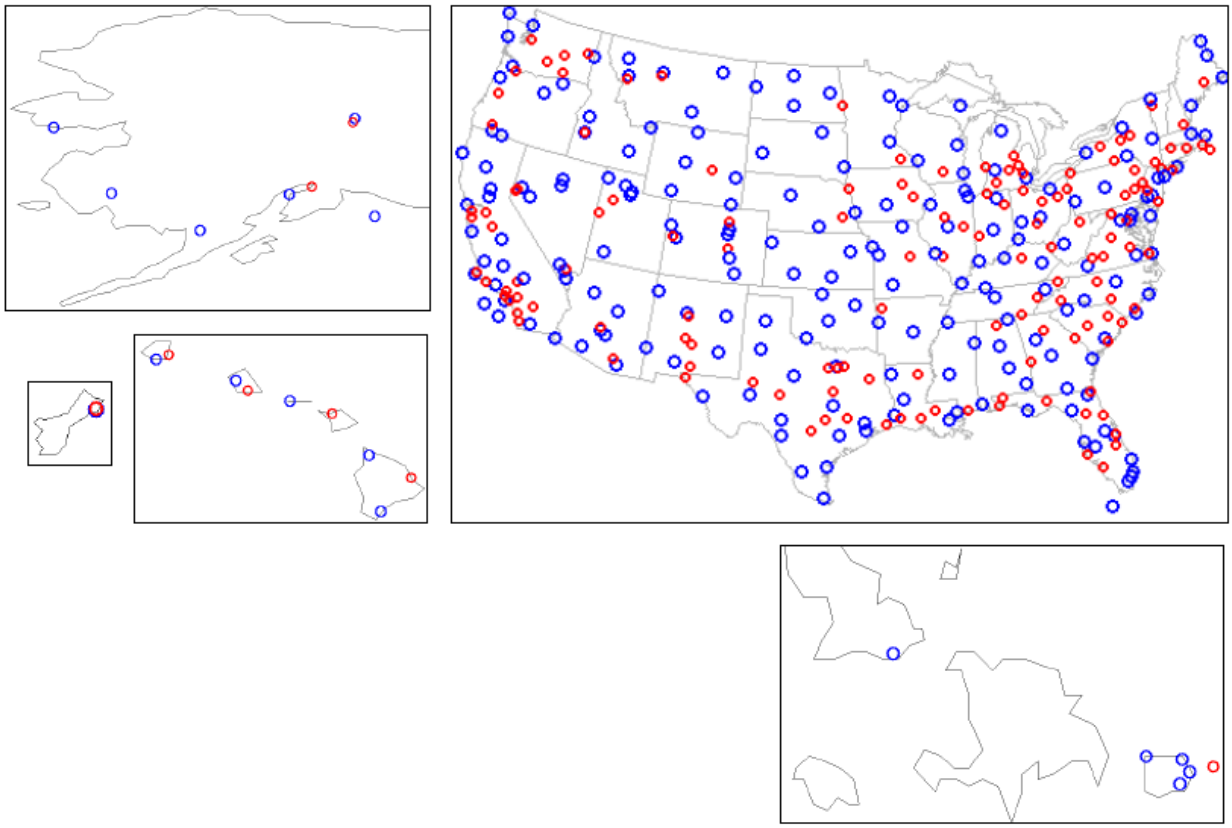

Figure 3-3. Locations of MPAR (blue) and TMPAR (red) for Scenario 3. Clockwise from top left: Alaska, contiguous United States, Puerto Rico/Virgin Islands/Guantanamo Bay, Hawaii, and Guam.

The numbers of relevant radars for each scenario are shown in Table 3-1. In the siting analysis, some of the radars were assigned to have less than four antenna faces in an attempt to minimize cost while maintaining the required coverage. In order to reduce the complexity of the problem and to be conservative, we will assume that all MPARs and TMPARs have four faces for the frequency assignment exercise. The total number of legacy S-band radars (ASRs and NEXRADs) is 387, so the total will either stay the same (Scenario 1) or decrease (Scenarios 2 and 3). Note that the U.S. military operates tactical surveillance radars in the same band; however, we will not include them in this initial study as they are relocatable and their frequency assignments are classified.

TABLE 3-1
Number of Radars Included in Analysis

Scenario	NEXRAD	MPAR	TMPAR	Total
1	156	43	188	387
2	0	174	139	313
3	0	218	148	366

The main input to the frequency analysis program is a file containing the following data for each potential radar site:

(a) latitude and longitude of the radar site,
(b) elevation of the site,
(c) height of the site antenna (approximated by the antenna tower height),
(d) type of radar at this site for each scenario (0 = no radar, 1 = MPAR, 2 = TMPAR, 3 = NEXRAD), and
(e) operating frequency band (if radar is a NEXRAD).

This frequency analysis program calls a function that determines whether the transmitting radar will interfere with the receiving radar. Quantitatively, interference is deemed to exist if the interference signal to noise ratio (INR) in the receiver exceeds a specified threshold. Studies have shown that the INR at which radar target detection and data quality become noticeably affected is dependent on the duty cycle of the interfering transmitter (Sanders et al., 2006). Whereas interference from communication devices (~100% transmission duty cycle) impacts receiving radar data at an INR of –6 dB, pulsed radars transmitting at duty cycles of less than 1–3% are tolerable up to INRs as high as 30–63 dB. In fact, RSEC Section D requires receiver tolerance of INR <50 dB against pulsed radars with duty cycles up to 0.8% (NTIA, 2011), and ASR-11 specifications call for meeting detection requirements in the presence of peak INR ≤ 75 dB with duty cycles up to 0.9% (Raytheon, 1999). We shall proceed under the assumption that future phased array radars would also be subject to the same RSEC Section D requirement (although there are questions regarding how difficult this would be). Since the radars under consideration operate under a wide range of duty cycles (Table 2-1), we selected a maximum INR tolerance threshold of 50 dB for duty cycle <0.8%, an INR threshold of –6 dB for 100% duty cycle, and used interpolation to obtain INR thresholds for intermediate duty cycles.

The INR in dB units is given by

$$INR = P_t + G_t - L_p + G_r - L_r - P_n \,, \tag{3-1}$$

where Pt is peak power transmitted from the antenna, Gt is the transmitter antenna gain, Lp is the propagation loss, Gr is the receiver antenna gain, Lr is the receiver rejection loss, and Pn is the system noise power in the receiver bandwidth. In our analysis we considered the case where the transmitter and

receiver antennas are azimuthally aligned (main lobe-main lobe) and where they are not (main lobe-side lobe). In the former case, the antenna gains used will be the peak values for both transmit and receive minus 3 dB each. The 3 dB loss is included because the lowest elevation angle used operationally on these radars is typically half the elevation beamwidth so that the antenna pattern aimed at the horizon is the –3-dB point. An exception may be MPARs located around the perimeter of the country (in lieu of Air Route Surveillance Radar-4s (ARSR-4s)) that may scan down to negative elevation angles. But these would generally be looking outward along the national boundary and not toward other radars in this study. We include the main lobe-side lobe case, because if the MPARs and TMPARs are controlled as a network, it should be possible to ensure that main lobe-main lobe conflicts never arise during operation. Even for Scenario 1 with NEXRADs still deployed, if their azimuthal scan angles can be reported in real time, the MPARs and TMPARs may be able to adapt their scan strategies to avoid main lobe conflict with the NEXRADs. In a main lobe-side lobe case we decrease one of the antenna gains by 40 dB, which is the one-way far side lobe specification for the current weather radars (Appendix A).

The propagation loss includes the free-space loss, atmospheric attenuation, and terrain-dependent factors. The latter were computed using the Longley and Rice (1968) model with Level 1 Digital Terrain Elevation Data (DTED) as input. Average ground conductivity of 0.005 mho/m and permittvity $\varepsilon = 15$ (Rice et al., 1967) were assumed. Although both vertical and horizontal polarization would be used by the radars, vertical polarization was chosen for the propagation model, because it tends to decay slower over the Earth. An ellipsoid model of Earth was used for distance calculations with atmospheric refraction accounted for by the standard 4/3-Earth-radius model (e.g., Skolnik, 2008).

The Longley-Rice model breaks down the propagation problem into three distance regimes. At close range, two-ray (direct and ground-reflected) optics and diffraction effects are presumed to dominate. At very far range, forward scattering attenuation is predominant. At intermediate distances, diffraction effects are paramount. The model computes the transition ranges and applies the appropriate physics to each regime using the actual terrain elevation profile and the antenna heights above ground level. It is intended for use in the frequency range of 20 to 40,000 MHz and range of 1 to 2,000 km.

In Equation 3-1 the receiver loss term is, in general, dependent on the frequency mismatch between the transmitter and receiver. For the purposes of the frequency assignment program the two frequencies are assumed to be the same. We set the receiver loss to a nominal value of 2 dB to account for RF path loss.

There are several cases to be considered in the overall frequency analysis. A NEXRAD radar site uses a single transmit and receive frequency, while an MPAR or TMPAR radar site will transmit and receive two pulse types (no modulation and FM) on separate frequency channels. The rotating antenna of a NEXRAD makes the site omni-directional for the purposes of frequency allocation, while each MPAR or TMPAR radar site has four faces that could be operated together, in opposing pairs, or independently. In reality, a NEXRAD is assigned a second frequency channel for its redundant transmitter, but only one channel is in operation at any given time.

The simplest form of the frequency analysis process assumes that all the radar sites are either NEXRADs (rotating antenna) or MPAR/TMPARs with all four faces operated together. The frequency

analysis process associates an array of "frequency-in-use" flags for each potential radar site as read from the input file. The flag array has an entry for each possible frequency that might be required at a given radar site (presently sized for up to 100 frequencies). The entire flag array is initialized at start-up to "unused."

The frequency analysis process "outer loop" looks at each potential radar site in turn in the order that they were read from the input file. If this radar site is not included in the desired scenario then the processing continues with the next potential radar site from the file. Otherwise, the radar transmitter parameters for this site are set up for the interference determination function. The first unused frequency for the current radar site is found by scanning its "frequency-in-use" flags. This frequency is now marked as "in-use" for the current radar site and a search is made through all the remaining potential radar sites to find and mark all those sites that would be interfered with on this frequency.

The search for other sites is done one at a time through the list of radar sites in the input file. If this second radar site is not included in the desired scenario then the search processing continues with the next potential radar site from the file. Otherwise, the radar receiver parameters of the second radar site are set up for the interference determination function. If there is interference then this frequency is marked as "used" for the second radar site and the search processing continues until all the potential second radar sites have been checked and marked if necessary.

The frequency analysis process is complete when all of the potential radar sites from the input file have been checked in the "outer loop." The statistics of frequency allocation for this scenario are then generated in a second pass through all the potential radar sites. For each radar site, the number of frequencies used is computed by summing the number of frequency flags set for this radar site. The final output of the frequency analysis is a histogram of the number of radar sites for each non-zero number of frequencies.

MPAR and TMPAR radar sites are assumed to require two, four, or eight independent frequency channels (as listed in Table 2-2). This is handled in the frequency analysis process by treating each frequency as separate, co-located transmitting and receiving sites.

Dealing with the ability of MPAR and TMPAR radar sites to operate their four faces in synchronous, paired, or independent fashion adds some further complexity to the frequency analysis process. The MPAR/TMPAR paired-face radar sites are assumed to have sufficient isolation between their opposing faces to allow sharing of frequencies. The MPAR/TMPAR radar sites that use their four faces independently cannot share frequencies between the faces. The "frequency-in-use" flags array now requires an additional dimension for up to four radar faces. The final histogram generation step must sum the number of used frequencies for each site over all the radar faces of that site. The frequency count used for this radar site is now the maximum of the counts for each face. Each MPAR/TMPAR radar site is now treated as four (two frequencies per face pair) co-located sites (for the paired-face case) or eight (two frequencies per face) co-located sites (for the independent face case). A bearing-angle test is employed in addition to the interference test described in the search processing above.

The bearing-angle test employed in this frequency analysis makes simplifying assumptions. Every MPAR and TMPAR radar site is assumed to have its four faces aligned to north-east-south-west. For the main lobe-main lobe interference test cases, only the particular interferer radar face that the current radar site points to (or the particular interferer face pair including this face for the paired-face case) will be marked as used. For the main lobe-side lobe test cases, all four faces (or both face pairs) of the interferer radar site will be marked as used if the particular radar face of the current radar site points to the interferer site. The bearing-angle test used for the paired-face case is further illustrated in Figure 3-4. For the given geometry between Radar 1 (blue) and Radar 2 (red), there is potential main lobe-main lobe interference only between frequencies B1 and B2. For main lobe-side lobe interaction, there is potential interference between the frequency pairs (B1 A2), (B1 B2), (B2 A1), and (B2 B1).

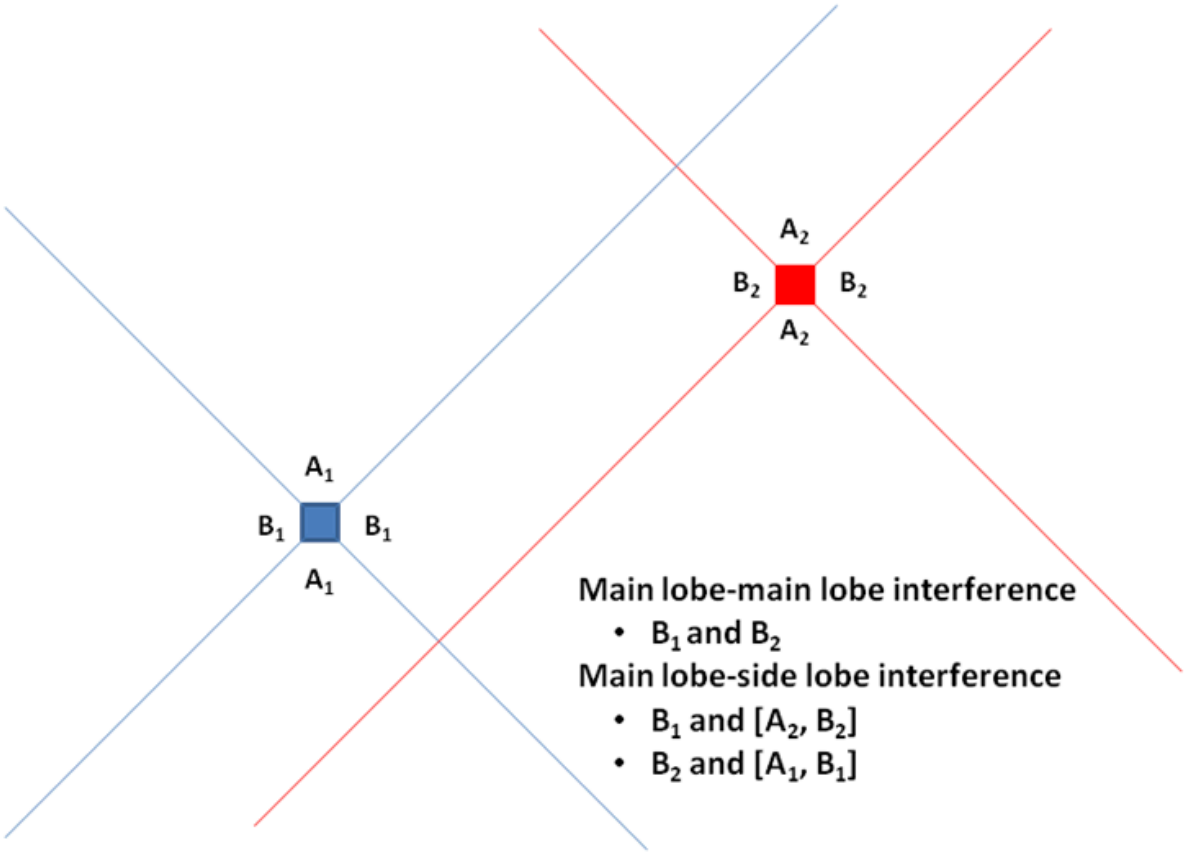

Figure 3-4. Bearing-angle test illustration for the paired-face case.

The bearing-angle test used for the case of four independent faces is illustrated in Figure 3-5. For the given geometry between Radar 1 (blue) and Radar 2 (red), there is potential main lobe-main lobe interference only between frequencies B_1 and D_2. For main lobe-side lobe interaction, there is potential interference between the frequency pairs (B_1 A_2), (B_1 B_2), (B_1 C_2), (B_1 D_2), (B_2 A_1), (B_2 B_1), (B_2 C_1), and (B_2 D_1).

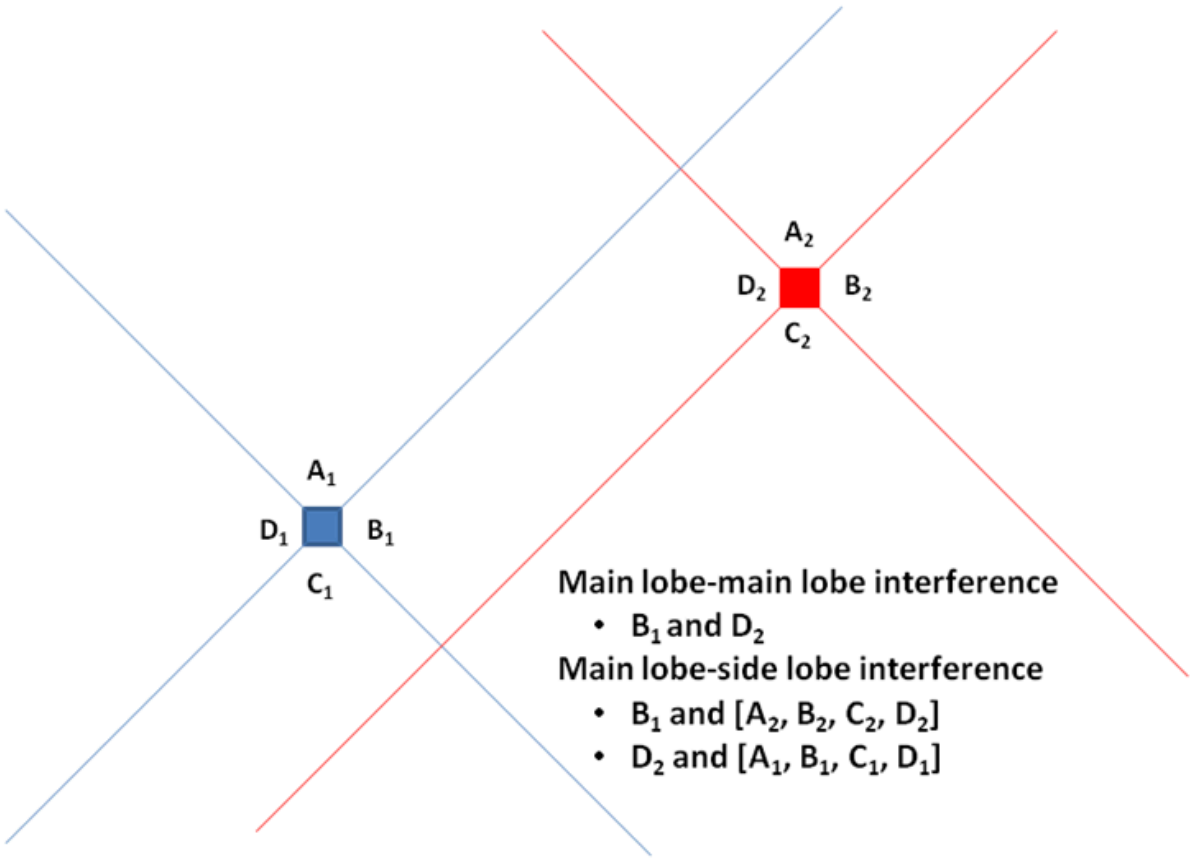

Figure 3-5. Bearing-angle test illustration for the four-independent-faces case.

3.1 SEQUENTIAL SCANNING CASE

First, we will study the situation where only sequential scanning is needed to accomplish all of MPAR's missions, and we will begin with the main lobe-main lobe interaction cases. Figure 3-6

illustrates the results of the frequency assignment for Scenario 1 where the 156 rotating-antenna single-frequency NEXRAD radar sites are retained. The NEXRAD/MPAR/TMPAR all-faces case required a total of 14 independent frequency channels (radar site KTBW in Ruskin, Florida used the maximum). The NEXRAD/MPAR/TMPAR paired-face case required seven frequency channels (radar site ONT in Ontario, California used the maximum). A total of eight frequency channels (the minimum possible) were required when the NEXRAD/MPAR/TMPAR radars had to assign a frequency pair to each of their four faces separately. The closest pair of radar sites included for this scenario was in Melbourne, Florida (TMPAR at MLB [ASR-11] and NEXRAD at KMLB) which are about 1.4 km apart.

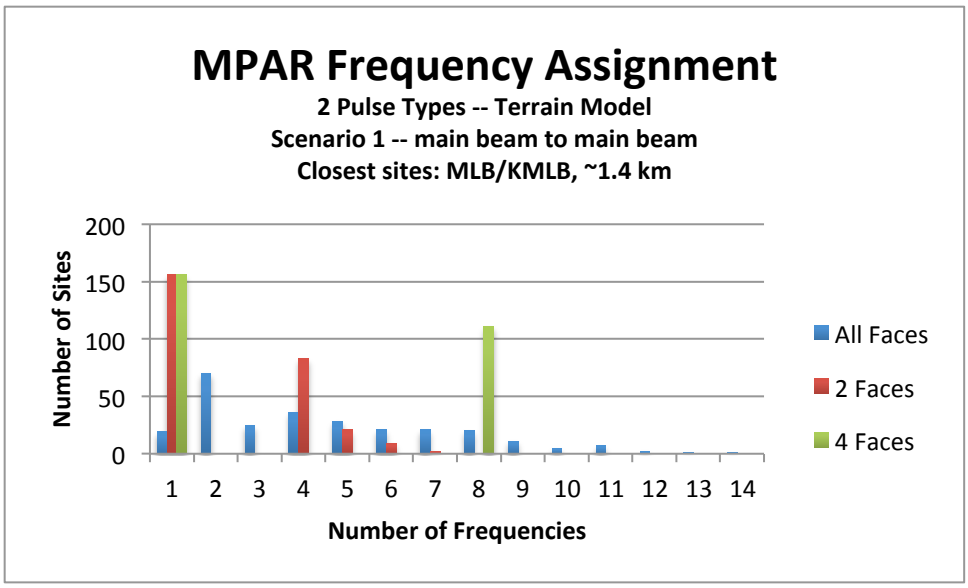

Figure 3-6. MPAR frequency assignment histogram for Scenario 1, main beam to main beam interaction, sequential scanning case.

Figure 3-7 illustrates the results of the frequency assignment for Scenario 2 where all the NEXRAD radar sites are replaced. The MPAR/TMPAR all-faces frequency allocation case required a total of 12 independent frequency channels (radar site TPA in Tampa, Florida used the maximum). The MPAR/TMPAR paired-face case required nine frequency channels (radar site KIWX in North Webster, Indiana used the maximum). A total of eight frequency channels (the minimum possible) were required when the MPAR/TMPAR radars had to assign a frequency pair to each of their four faces separately. Note that since each MPAR and TMPAR face requires a minimum of two independent frequencies for its operation (one with no pulse modulation and a second with FM modulation) there are no sites with a single frequency in the Scenario 2 histogram. The closest pair of radar sites included for this scenario was in Guam (TMPAR at UAM (ASR-8) and MPAR at PGUA (NEXRAD)), which are about 14.6 km apart.

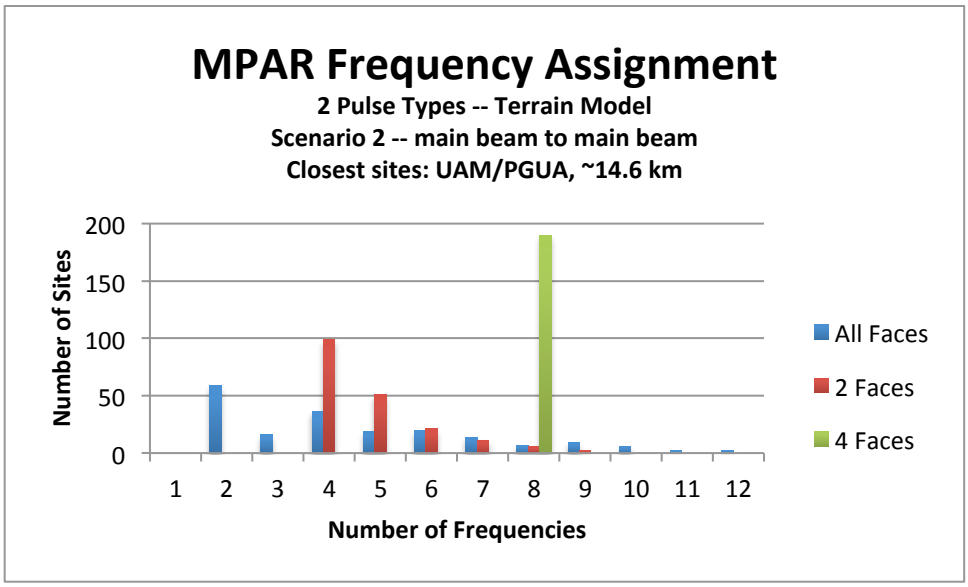

Figure 3-7. MPAR frequency assignment histogram for Scenario 2, main beam to main beam interaction, sequential scanning case.

Figure 3-8 illustrates the frequency assignment for Scenario 3 where there are more MPAR and TMPAR sites than were considered for Scenario 2. The MPAR/TMPAR all-faces case required a total of 18 independent frequency channels (radar site TPA used the maximum). The MPAR/TMPAR paired-face case required 12 frequency channels (radar site QLA in San Pedro, California used the maximum). A total of eight frequency channels (the minimum possible) were required when the MPAR/TMPAR radars had to assign a frequency pair to each of their four faces separately. The closest pair of radar sites included for this scenario was in Guam (TMPAR at UAM (ASR-8) and MPAR at QLR (ARSR-4)), which are about 0.5 km apart.

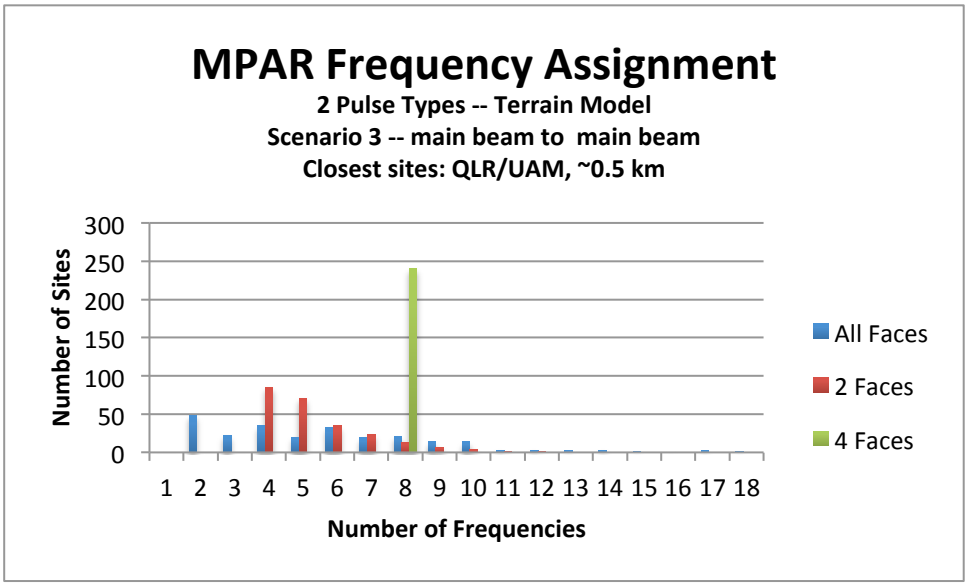

Figure 3-8. MPAR frequency assignment histogram for Scenario 3, main beam to main beam interaction, sequential scanning case.

Now we consider the main lobe-side lobe interaction cases. Figure 3-9 parallels Figure 3-6 for Scenario 1, except that the "main beam to main beam" interference flag parameter is set false. The NEXRAD/MPAR/TMPAR all-faces case required five independent frequency channels (radar site KLOT in Romeoville, Illinois used the maximum). The NEXRAD/MPAR/TMPAR paired-face case required six frequency channels. A total of 10 frequency channels were required when the NEXRAD/MPAR/TMPAR radars had to assign a frequency pair to each of their four faces separately. (Radar site PNS in Pensacola, Florida used the maximum for the paired-face and four-face cases.)

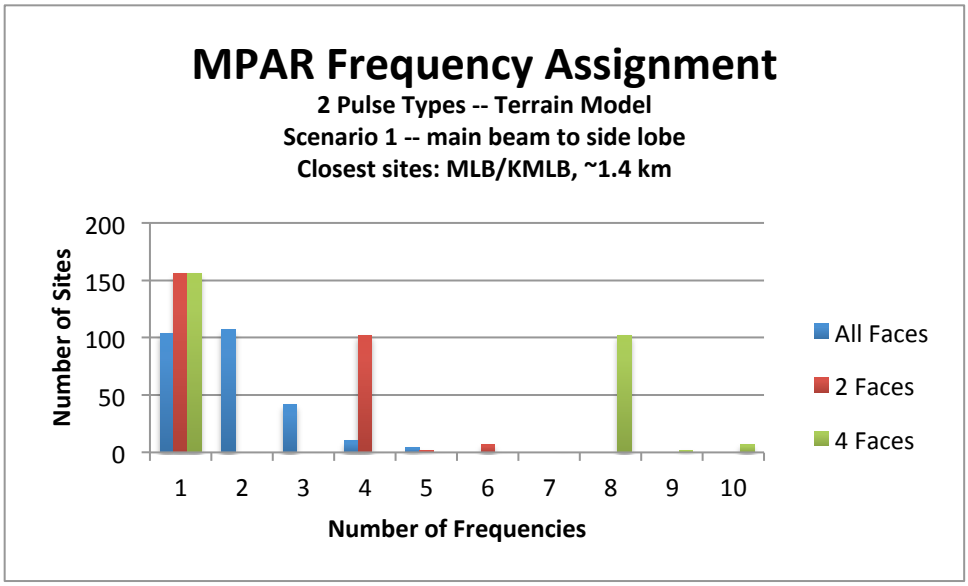

Figure 3-9. MPAR frequency assignment histogram for Scenario 1, main beam to side lobe interaction, sequential scanning case.

Figure 3-10 parallels Figure 3-7 for Scenario 2, except that the "main beam to main beam" interference flag parameter is set false. The MPAR/TMPAR all-faces case required six independent frequency channels (radar site KDIX in Fort Dix, New Jersey used the maximum). The MPAR/TMPAR paired-face case required seven frequency channels (radar site PNS used the maximum). A total of 12 frequency channels were required when the MPAR/TMPAR radars had to assign a frequency pair to each of their four faces separately (radar site KDIX used the maximum).

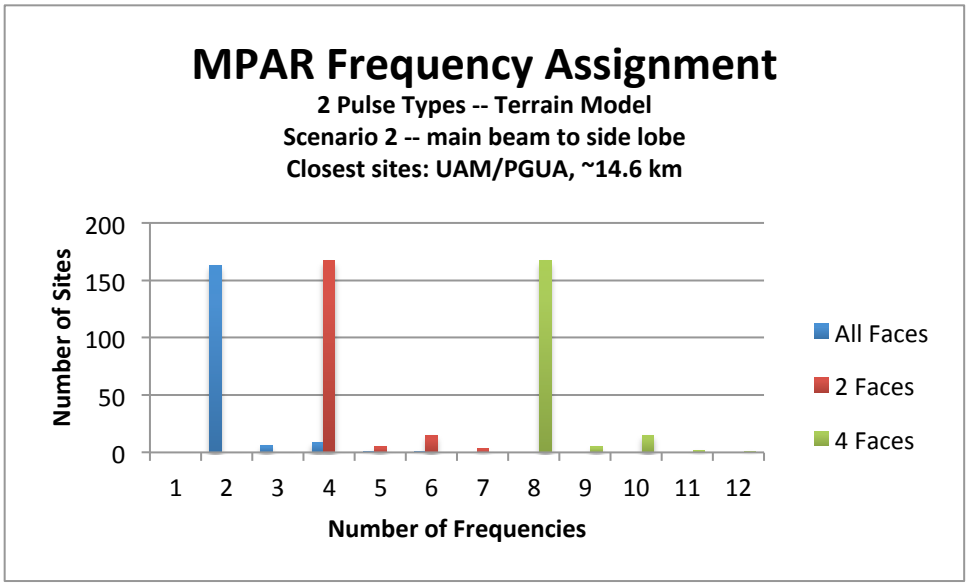

Figure 3-10. MPAR frequency assignment histogram for Scenario 2, main beam to side lobe interaction, sequential scanning case.

Figure 3-11 parallels Figure 3-8 for Scenario 3, except that the "main beam to main beam" interference flag parameter is set false. The MPAR/TMPAR all-faces case required seven independent frequency channels (radar site QLA used the maximum). The MPAR/TMPAR paired-face case required nine frequency channels (radar site NKX at Miramar Marine Corps Air Station, California used the maximum). A total of 14 frequency channels were required when the MPAR/TMPAR radars would assign a frequency pair to each of their four faces separately (radar site NKX used the maximum).

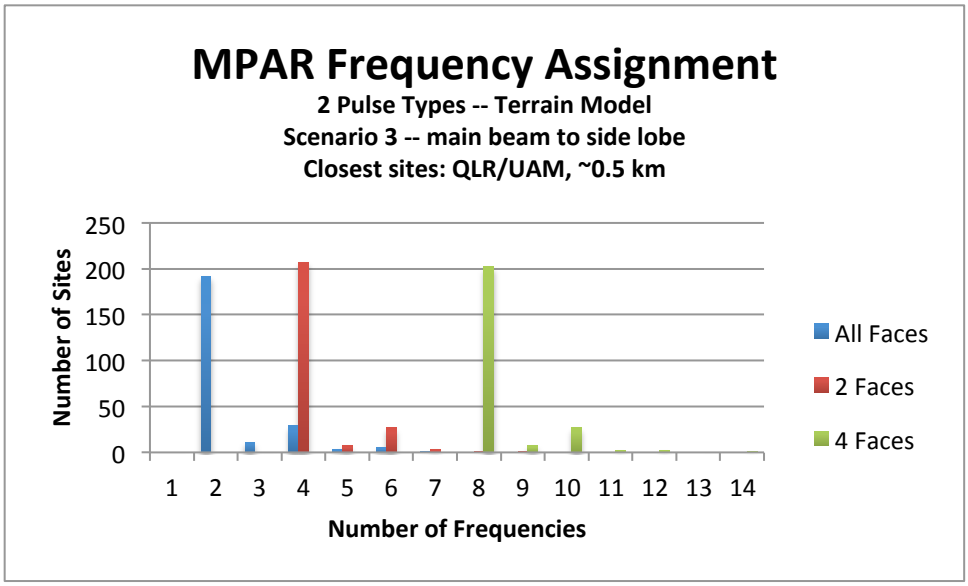

Figure 3-11. MPAR frequency assignment histogram for Scenario 3, main beam to side lobe interaction, sequential scanning case.

Table 3-2 below summarizes the results of the MPAR frequency allocation analysis for sequential scanning. The number of required frequencies is indicated for each of the three scenarios, the four MPAR configurations, and the selection of main lobe-main lobe or main lobe-side lobe interaction. For main lobe-main lobe interaction, the required number of frequencies is highest for the all-faces (omnidirectional) case. This is because even though the number of frequencies used per radar is smallest for this case, the number of other radars that a given radar may interfere with is largest. Interestingly, the opposite is true for main lobe-side lobe interaction—the four faces operating independently case requires the largest number of frequencies. This is because, as can be seen from Figure 3-5, the number of frequency channels of other radars that a given radar face may interfere with is increased four-fold relative to main lobe-main lobe interaction.

TABLE 3-2
Number of Required MPAR Frequencies for Sequential Scanning Case

Interaction Type	MPAR Configuration	Scenario		
		1	2	3
Main lobe-main lobe	All Faces	14	12	18
Main lobe-main lobe	2 Faces	7	9	12
Main lobe-main lobe	4 Faces	8	8	8
Main lobe-side lobe	All Faces	5	6	7
Main lobe-side lobe	2 Faces	6	7	9
Main lobe-side lobe	4 Faces	10	12	14

Table 3-3 below parallels Table 3-2. The radar site that required the largest number of frequencies for the particular allocation strategy is noted for each scenario, MPAR configuration, and interaction type. If more than one radar site required the maximum number of frequencies, the first site found in the scenario database is noted. The exception is the third row of Table 3-3, where all sites have the same (8) number of frequencies.

TABLE 3-3
Radar Sites Requiring Most MPAR Frequencies for Sequential Scanning Case

Interaction Type	MPAR Configuration	Scenario		
		1	2	3
Main lobe-main lobe	All Faces	KTBW	TPA	TPA
Main lobe-main lobe	2 Faces	ONT	KIWX	QLA
Main lobe-main lobe	4 Faces	All	All	All
Main lobe-side lobe	All Faces	KLOT	KDIX	QLA
Main lobe-side lobe	2 Faces	PNS	PNS	NKX
Main lobe-side lobe	4 Faces	PNS	KDIX	NKX

We believe that with the agile and adaptive beam pointing capability of MPAR together with real-time network connections to the other radars, main lobe-main lobe interactions can be avoided. Therefore, the worst-case scenario for sequential scanning would be the case of four faces operating independently (the final row of Tables 3-2 and 3-3). We assume that the available spectrum window is 200 MHz (2.7 to 2.9 GHz) for Scenario 1, because only the ASRs' frequency band would be made available to MPAR. For Scenarios 2 and 3 we assume that 300 MHz (2.7 to 3.0 GHz) would be available, since that is the band occupied by NEXRAD, which will be replaced in those scenarios. Thus, the worst cases to examine would be the 10 frequencies needed at PNS for Scenario 1 (for an average of 200 MHz/10 = 20 MHz per channel availability), and the 14 frequencies needed at NKX for Scenario 3 (for an average of 300 MHz/14 = 21.4 MHz per channel availability).

How far apart a transmitter and receiver must be in frequency in order to avoid interference depends on their spatial separation. The exact relationship will be affected by the terrain under the propagation path, but it is instructive to show results for a representative situation. In Figure 3-12 we present plots of minimum required frequency offset vs. distance for an interdecile terrain height deviation range of 30 m ("slightly rolling plains" in the Longley-Rice model), transmitter and receiver antenna height of 25 m, and main lobe-side lobe interaction. (For reference, the antenna tower height is 9 m at PNS and 23 m at NKX.) The spectral characteristics of the transmitted pulse and receiver given in Section 2 for the different radars are assumed. We see that the worst-case scenarios are easily accommodated as the minimum required frequency separation for all radars except NEXRAD is ≤20 MHz at 1 km separation distance. For NEXRAD, it is ≤20 MHz at 4 km range. The nearest radar to PNS (TMPAR at Pensacola, Florida) is NSC (TMPAR at Whiting Field Naval Air Station, Florida), which is 50 km away. The closest radar to NKX (TMPAR at Miramar Marine Corps Air Station, California) is NFG (TMPAR at Camp Pendleton, California), which is 48 km away.

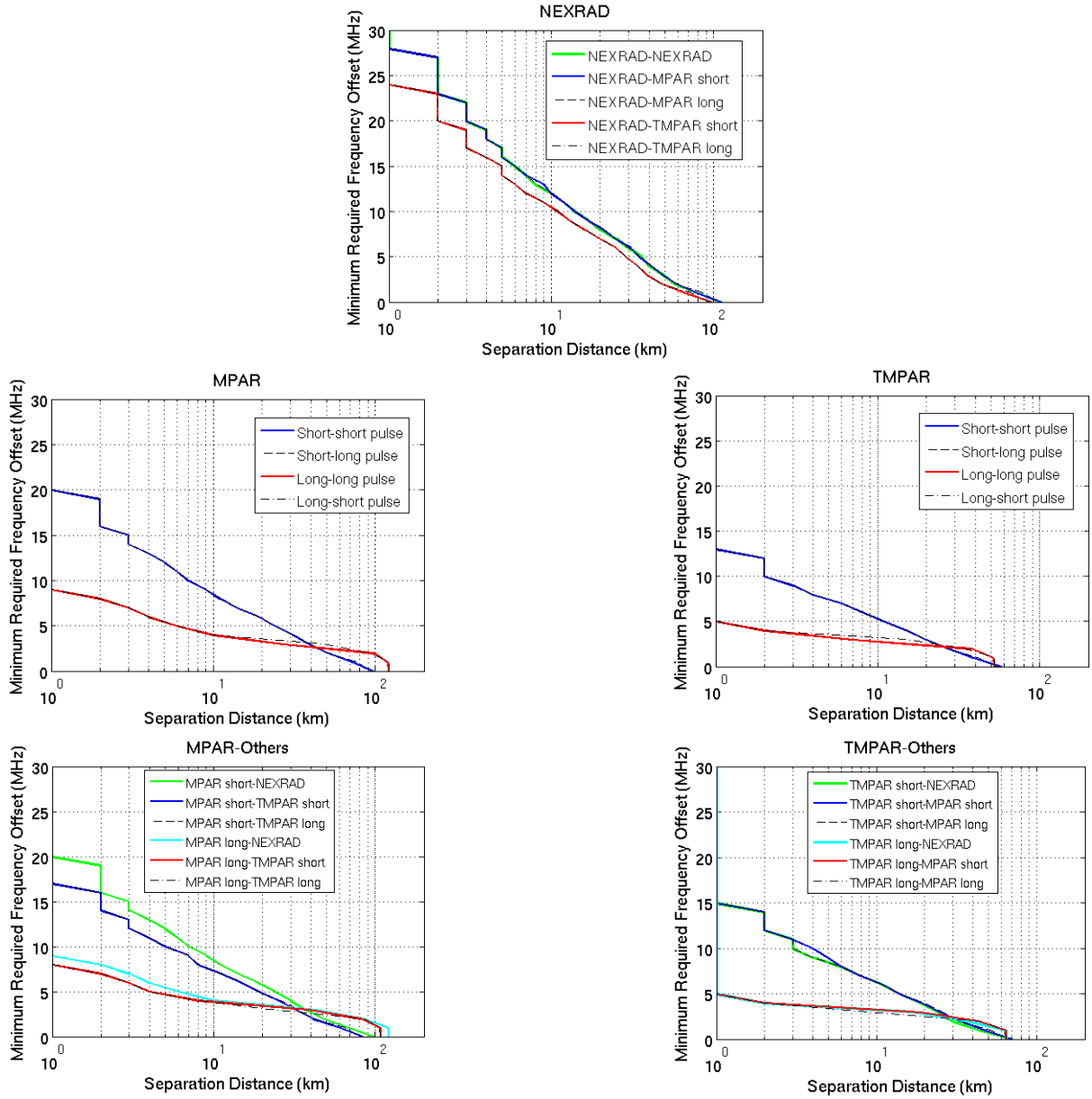

Figure 3-12. Plots of minimum required transmit-receive frequency offset vs. separation distance for interference avoidance. Main lobe to side lobe interaction is assumed. The first panel shows results for NEXRAD as the transmitter and other radar types as the receiver. The next two panels show results for transmission and reception by the same radar type (MPAR or TMPAR). The last two panels show results with transmission by MPAR/TMPAR and reception by other radar types. The inset legends indicate the transmission-reception pulse mode combinations.

3.2 PARALLEL SCANNING CASE

The MPAR frequency analysis discussed thus far has assumed that surveillance and weather functions could be time-shared on a single frequency. (Technically, a pair of frequencies to provide isolation between the short and long pulse modes.) The impact on frequency requirements if this assumption is false will be explored here. We will consider the cases where scanning would take place in parallel across two and three independent frequencies. In the former case, the difference from the sequential scanning case where two frequencies were needed for the short- and long-pulse modes, is that now the short and long pulses could be transmitted and received in either channel. Therefore, the worst case for co-channel interference (the FM long pulse) must be assumed for both frequencies. For the case of three parallel frequencies, we simply add a third channel in the analysis.

As we believe that main lobe-main lobe interactions could be avoided in the MPAR concept of operations, we restrict our analysis to main lobe-side lobe interaction. Also, the "all faces" case will be skipped, since the number of frequencies that it requires is less than for the other cases under main lobe-side lobe interaction.

Figures 3-13 and 3-14 below provide the results of the frequency allocation analysis for Scenario 1. With two frequencies per MPAR/TMPAR face in Figure 3-13, the two faces allocation required six frequencies, and the four faces allocation required 10 frequencies. With three frequencies per MPAR/TMPAR face in Figure 3-14, the two faces allocation required nine frequencies, and the four faces allocation required 15 frequencies. The radar site PNS used the maximum number of frequencies for all cases.

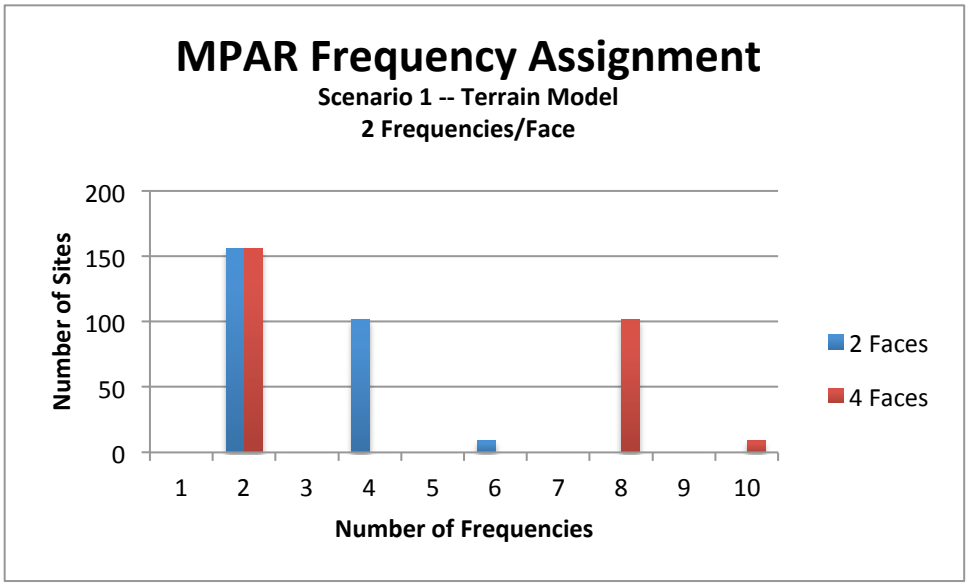

Figure 3-13. MPAR frequency assignment histogram for Scenario 1, main beam to side lobe interaction, parallel scanning on two frequencies per face case.

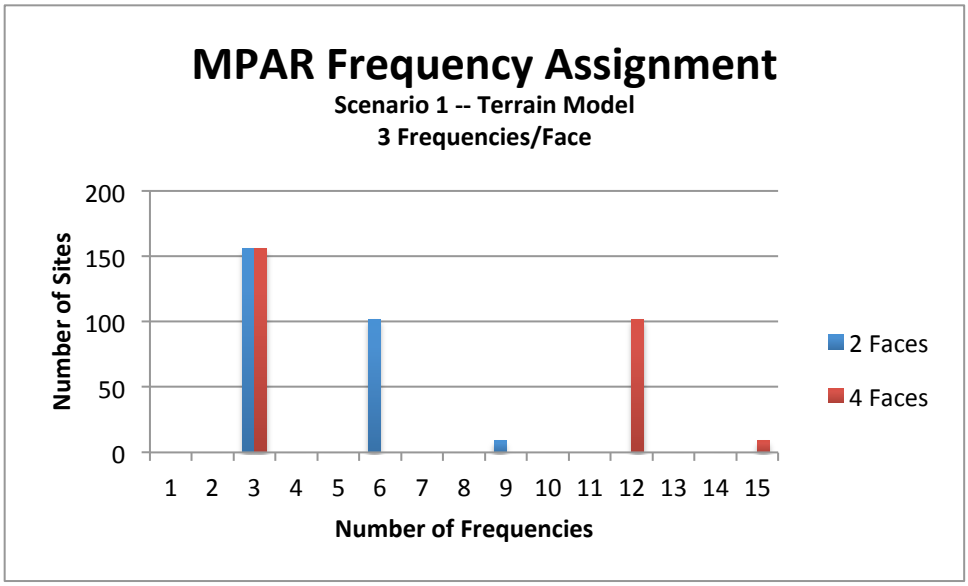

Figure 3-14. MPAR frequency assignment histogram for Scenario 1, main beam to side lobe interaction, parallel scanning on three frequencies per face case.

Figures 3-15 and 3-16 below provide the results of the frequency allocation analysis for Scenario 2. With two frequencies per MPAR/TMPAR face in Figure 3-15, the two faces allocation required eight frequencies, and the four faces allocation required 12 frequencies. With three frequencies per MPAR/TMPAR face in Figure 3-16, the two faces allocation required 12 frequencies, and the four faces allocation required 18 frequencies. The radar site KDAX in Davis, California used the maximum number of frequencies for all cases.

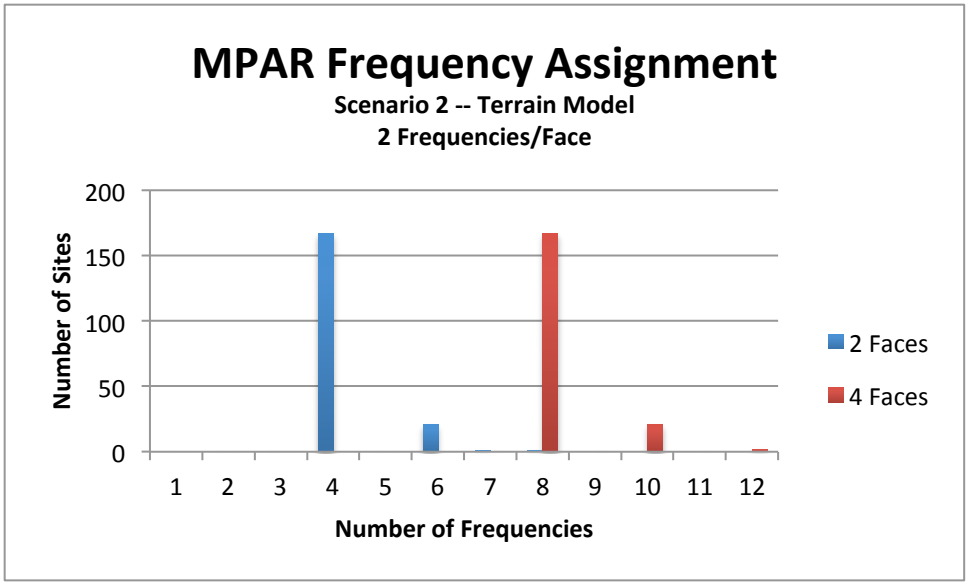

Figure 3-15. MPAR frequency assignment histogram for Scenario 2, main beam to side lobe interaction, parallel scanning on two frequencies per face case.

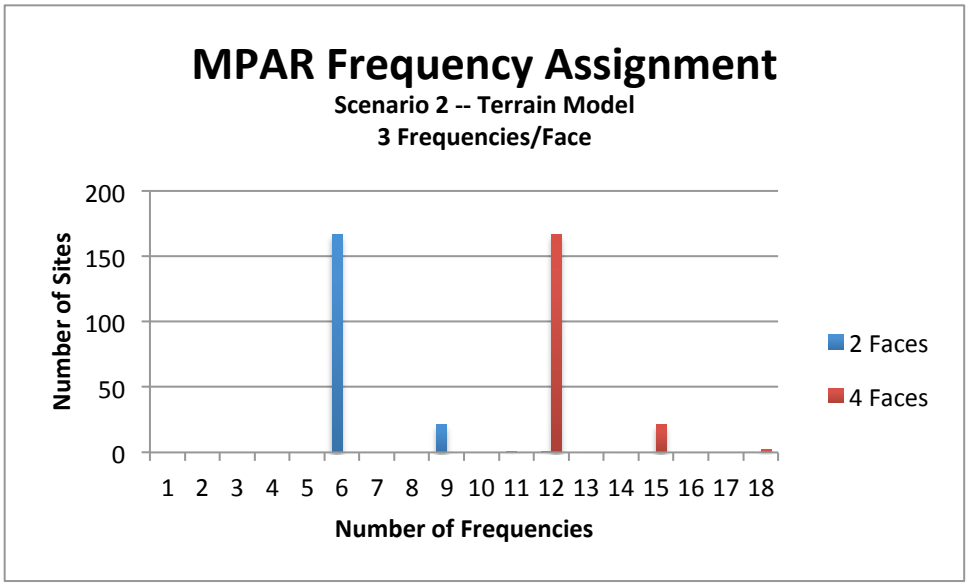

Figure 3-16. MPAR frequency assignment histogram for Scenario 2, main beam to side lobe interaction, parallel scanning on three frequencies per face case.

Figures 3-17 and 3-18 below provide the results of the frequency allocation analysis for Scenario 3. With two frequencies per MPAR/TMPAR face in Figure 3-17, the two faces required nine frequencies, and the four faces allocation required 14 frequencies. With three frequencies per MPAR/TMPAR face in Figure 3-18, the two faces allocation required 13 frequencies, and the four faces allocation required 20 frequencies. The radar site NKX used the maximum number of frequencies for all cases.

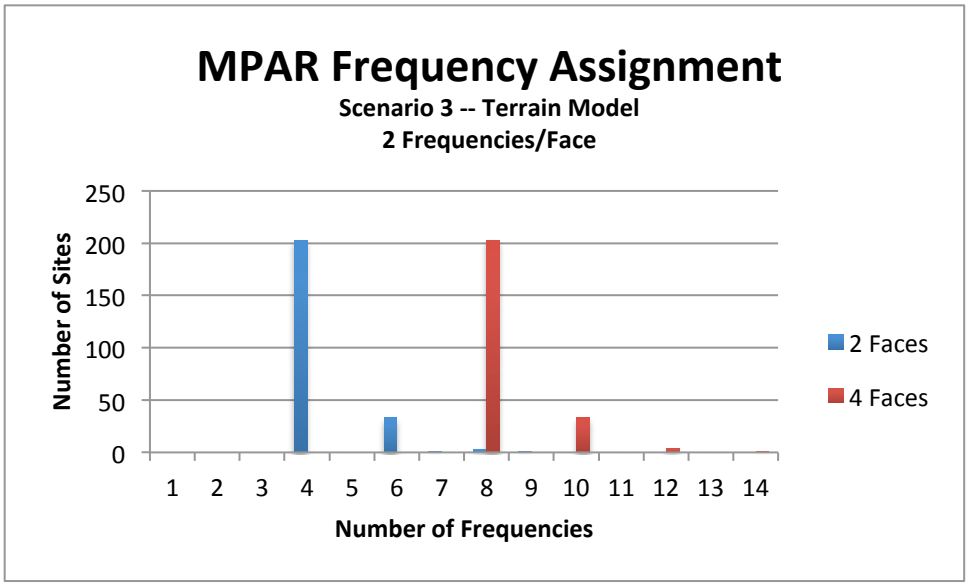

Figure 3-17. MPAR frequency assignment histogram for Scenario 3, main beam to side lobe interaction, parallel scanning on two frequencies per face case.

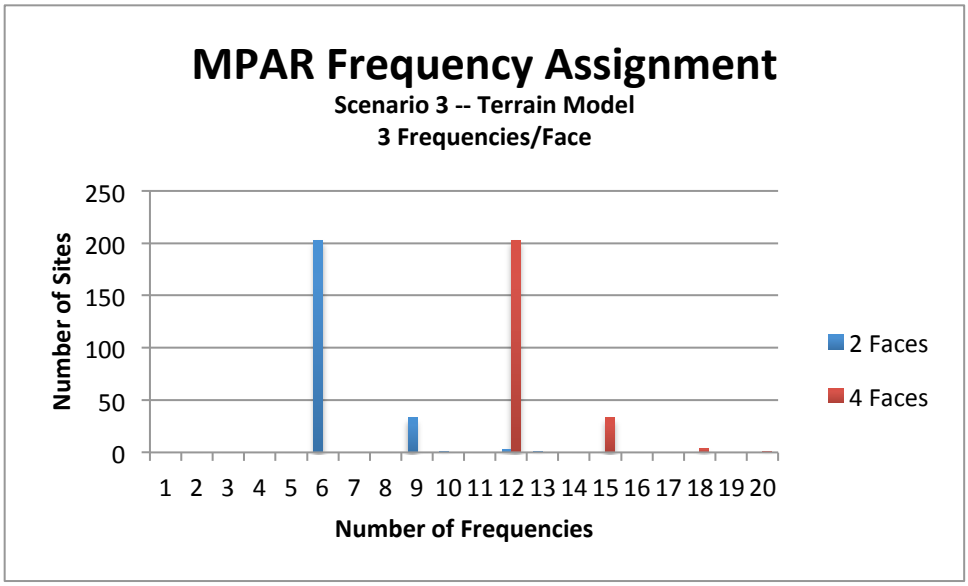

Figure 3-18. MPAR frequency assignment histogram for Scenario 3, main beam to side lobe interaction, parallel scanning on three frequencies per face case.

Table 3-4 below summarizes the results of the parallel scanning MPAR frequency allocation analysis for two frequencies per face and three frequencies per face. The number of required frequencies is indicated for each of the three scenarios, and the two-face and four-face MPAR configurations.

TABLE 3-4
Number of Required MPAR Frequencies for Parallel Scanning Case

Number of Frequencies per Face	MPAR Configuration	Scenario		
		1	2	3
2	2 Faces	6	8	9
2	4 Faces	10	12	14
3	2 Faces	9	12	13
3	4 Faces	15	18	20

Table 3-5 below parallels Table 3-4. The radar site that required the largest number of frequencies for the particular allocation strategy is noted for each scenario, MPAR configuration, and number of frequencies per face.

TABLE 3-5
Radar Sites Requiring Most MPAR Frequencies for Parallel Scanning Case

Number of Frequencies per Face	MPAR Configuration	Scenario		
		1	2	3
2	2 Faces	PNS	KDAX	NKX
2	4 Faces	PNS	KDAX	NKX
3	2 Faces	PNS	KDAX	NKX
3	4 Faces	PNS	KDAX	NKX

Comparing the two-frequencies-per-face cases for parallel scanning (Table 3-4) and sequential scanning (Table 3-2), we see that the only difference is the increase from 7 to 8 for Scenario 2, two faces configuration. Therefore, the conclusion reached for the sequential scanning case applies here: The maximum required number of frequencies can be accommodated by the available spectral space.

For three frequencies per face, the worst cases to examine are the 15 frequencies needed at PNS for Scenario 1 (for an average of 200 MHz/15 = 13.3 MHz per channel availability), and the 20 frequencies needed at NKX for Scenario 3 (for an average of 300 MHz/20 = 15 MHz per channel availability). From Section 3.1, we know that the nearest radar to PNS in Scenario 1 is 50 km away, and the closest radar to NKX in Scenario 3 is 48 km away. At 48 km, Figure 3-12 shows that the required frequency separation between any two radars is well under 5 MHz. Therefore, the maximum required number of frequencies can be handily contained within the available spectral space, even for parallel scanning with three frequencies.

We can see that, for any of the cases that we considered, there is substantial spectral space remaining for other radars not included in this initial study. A more complete analysis should take into account all other radars (such as military tactical systems) that operate in the same band. Furthermore, a more detailed site-by-site spectral allocation analysis would have to be conducted in conjunction with an MPAR deployment plan that specifies the exact locations of the new (or temporary) radars during the transition period when both legacy and new radars will be operating simultaneously.

With parallel scanning on multiple frequency channels per antenna face, it is unlikely that interference can be avoided between channels on the same face. The result would be "dead" gates on channels that are in receive mode at the same time that transmission occurs on another channel (Figure 3-19). There will be a corresponding degradation in performance associated with the data loss. Thus, there is a trade off between radar sensitivity (tied to the duty cycle) and the number of independent data samples available per dwell (tied to the dead gates). Since both factors contribute in the end to the data quality, there are optimal values of duty cycle (and, hence, maximum pulse length and pulse compression ratio) for weather and aircraft surveillance. This problem has been analyzed in a previous study for the three-frequency MPAR case (Cho, 2006).

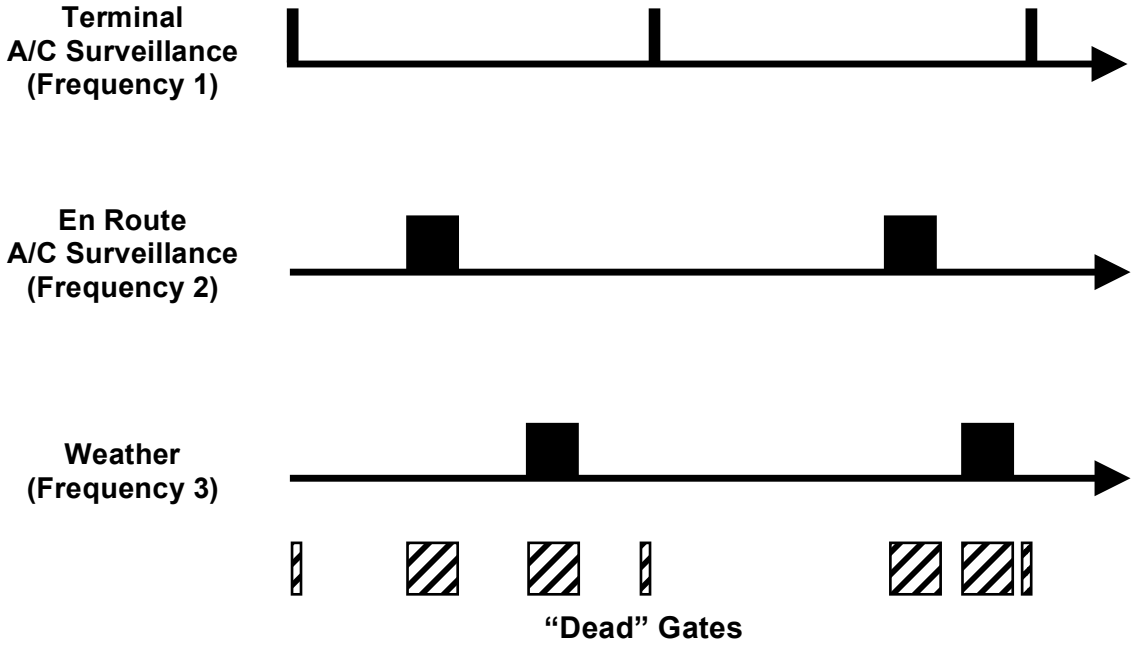

Figure 3-19. Illustration of cross-channel interference in an MPAR using parallel scanning with three frequency channels per antenna face.

How much interference we can expect (and be able to avoid) between different antenna faces on a single MPAR or TMPAR is another key question to examine. The answer will tell us which of the three operational choices given in Table 2-2 will be feasible. This issue is addressed in the next section.

4. INTERFERENCE BETWEEN ANTENNA FACES

Operation of MPAR with asynchronous pulsing on each face without dead gates is investigated in this section. In short, complete asynchronous operation without any interaction between faces is highly unlikely. However, beyond just a few of the worst cases lies a generally well behaved, very usable asynchronous operation region. This analysis is only a preliminary investigation into the feasibility and will focus on clutter returns from the ground below the MPAR tower. This study will not address diffraction from the edges of the radome, the edges of the faces, or the tower structure. This issue may be more limiting than ground clutter; however, methods of limiting diffraction and improving isolation have been developed (Balanis, 2005). A more detailed look into diffraction requires assumptions about the tower, radome, faces, etc., and using electromagnetic analysis. Instead we will focus on the general clutter problem that all tower-based phased arrays need to handle, and assess the feasibility of asynchronous operation of MPAR's located next to airfields.

The geometry of the face-to-face clutter coupling problem under consideration is shown in Figure 4-1. The main lobe to main lobe case happens when both faces are pointed in the same direction, at the 45^{o} point with one face transmitting and the second receiving (Figure 4-1). The two main lobes pointed in the same direction is unlikely to be usable as we will see later, and therefor, we will focus on the more general case of the transmit mainlobe to receive sidelobe coupling.

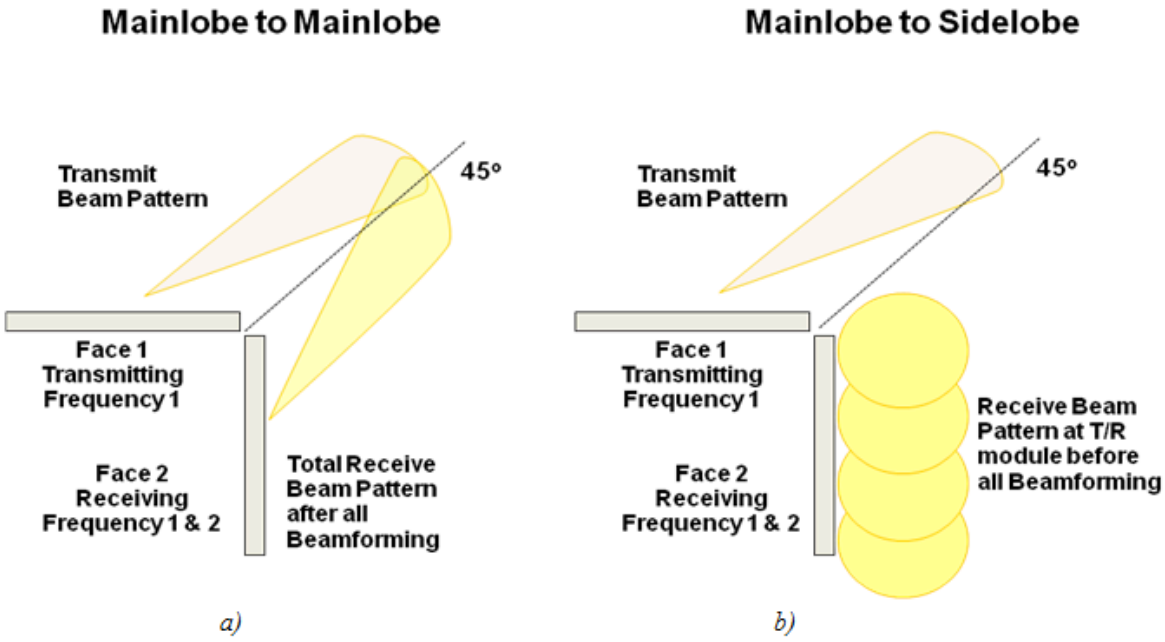

Figure 4-1. Geometry of interaction: a) Main lobe to main lobe interaction, receive beam shown after all beamforming. b) Main lobe to side lobe with the receive pattern of individual antenna beam patterns before beamforming.

As Figure 4-1 implies, the receive beam pattern for a phased array depends on where it is defined. A block diagram view of this is shown in Figure 4-2. For example, the receive beam pattern at each antenna element is a very broad pattern (~90°). After several levels of beamforming (analog and digital), we get the narrow beam pattern associated with the whole aperture. The amount of power the receive channel needs to handle (or the linearity) depends on where in the architecture it is defined. Therefore, to keep the analysis general, only the front end of the transmit/receive (T/R) module is investigated. After the analog beam combining significant reductions in linearity are seen in the sidelobe region. The strict mainlobe to mainlobe case in Figure 4-1a would have extreme linearity requirements, and as will be shown later, would only provide a few percent improvement over the mainlobe to sidelobe case.

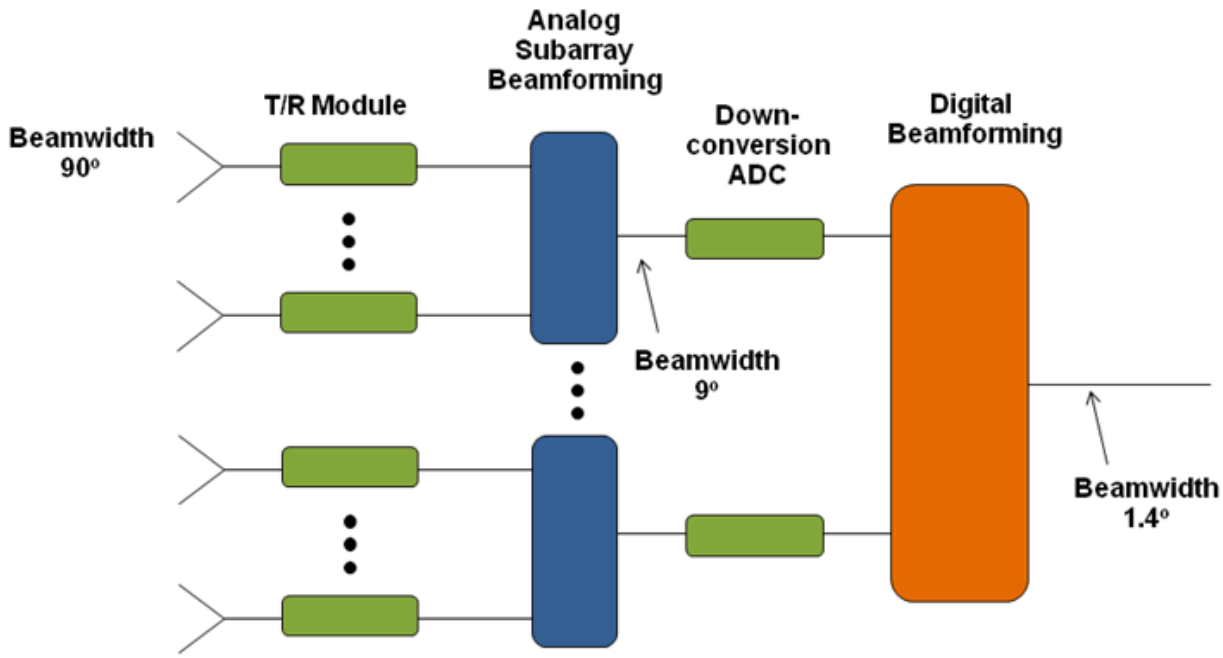

Figure 4-2. Block diagram of digital subarray architecture with representative beamwidths at various locations in receive chain.

4.1 TMPAR ANALYSIS

The transmit pattern of a TMPAR is calculated using an ideal uniform excitation and pointed at the horizon. The calculated pattern is shown in Figure 4-3. Also shown in the figure is the wide angle of the receive antenna element. The –90° angle is defined as looking straight down at the ground and 0° is defined as looking at the horizon. The most challenging case will be seen to be the case of the radar looking straight down since the range is only the height of the antenna over the ground (15 m for TMPAR and 30 m for full-sized MPAR). Note that both antenna patterns are idealized, and that the behavior at –90° is very difficult to model accurately without doing a full-wave analysis and including all diffraction, polarization, and mechanical errors.

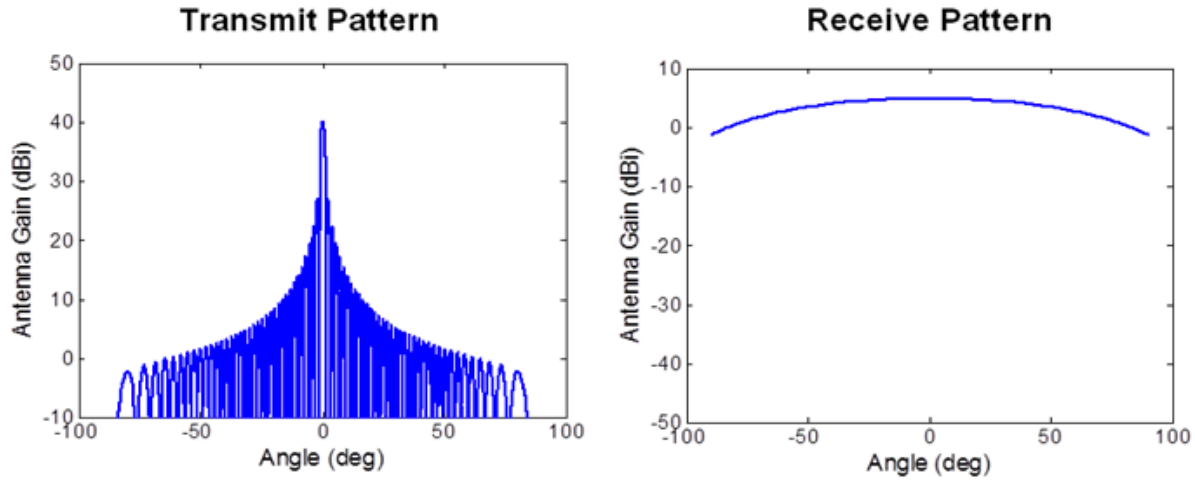

Figure 4-3. Ideal elevation patterns pointed at horizon. Transmit pattern is for 78 elements at 0.475λ spacing (corresponding to linear dimension of a 4 m × 4 m aperture), where λ is the radar wavelength. Receive pattern is for a single element.

The MPAR site is assumed to be free of buildings, fences, and other obstructions for this preliminary analysis. As we shall see, the first 50 m from the tower is the main problem for clutter. In contrast, many ASR-9 sites as the one shown from Google Maps at Logan Airport in Boston, Massachusetts in Figure 4-4 have buildings located coincident with the antenna tower. A clutter return from these structures could be added in a more detailed study for nearby scattering.

Figure 4-4. ASR-9 site at Logan International Airport in Boston, Massachusetts.

The TMPAR is assumed to be placed 15 m over grassland as shown notionally in Figure 4-5. We apply a clutter model (Ulaby, 1980) to the region illuminated by the transmit side lobes from one face and calculate the amount of power that enters each of the antenna elements at the second face. The equation for clutter power (Skolnik, 2008) is given as

$$C = \frac{P_t G_t G_r \lambda^2 \theta_B \sigma_0 \left(\frac{c\tau}{2}\right) \sec\phi}{(4\pi)^3 R^4}, \tag{4-1}$$

where c is the speed of light, τ is the pulse length, ϕ is the depression angle, and R is range. Some of the parameters were given in Table 2-1. The receive gain is that of a single element and is assumed to have a peak value of 5 dBi and a value of 3.5 dBi at 45° as shown in the geometry of Figure 4-1. The transmit gain at the 45° scan is assumed to have a peak antenna gain of 39.5 dBi to account for a 1.5 dB reduction due to the scan angle. The θ_B is the azimuth (horizontal) beamwidth and is assumed to be 1.4°. The antenna gain is a function of angle as was shown in Figure 4-3, and this relation is used in the clutter power equation. The radar scattering cross-section per unit area σ_o is found from Ulaby (1980).

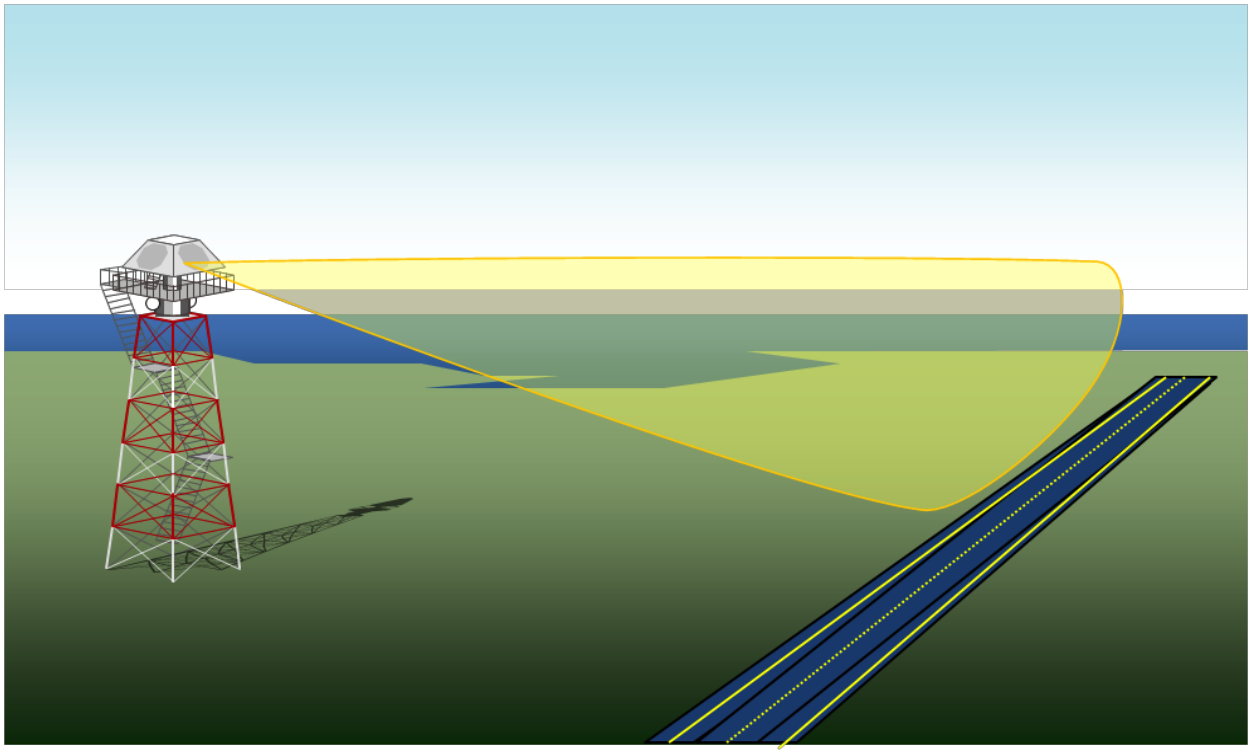

Figure 4-5. TMPAR at airport site. Grasslands assumed around TMPAR.

The clutter power returns using this approach led to a peak clutter return nearly directly below the tower as shown in Figure 4-6. The incoming power level of –13 dBm is relatively high. To understand the impact of this power level, a harmonic balance simulation using a commercial RF simulation tool (Agilent ADS 2009) was performed on a fairly typical T/R module receive specification gain of 24 dB and 3rd order output intercept point (OIP3) of 20 dBm. A desired received signal of 2.8 GHz at –110 dBm is entering the antenna element while a second frequency from the second face located at 2.84 GHz is simulated to see at what power the jamming signal affects the desired signal by 1 dB. Using these parameters, the jamming signal must be –17 dBm or less to keep the desired signal from being affected as shown in Figure 4-7. Clearly, even the best case transmit pattern leads to a situation with detrimental effects on the receive functionality.

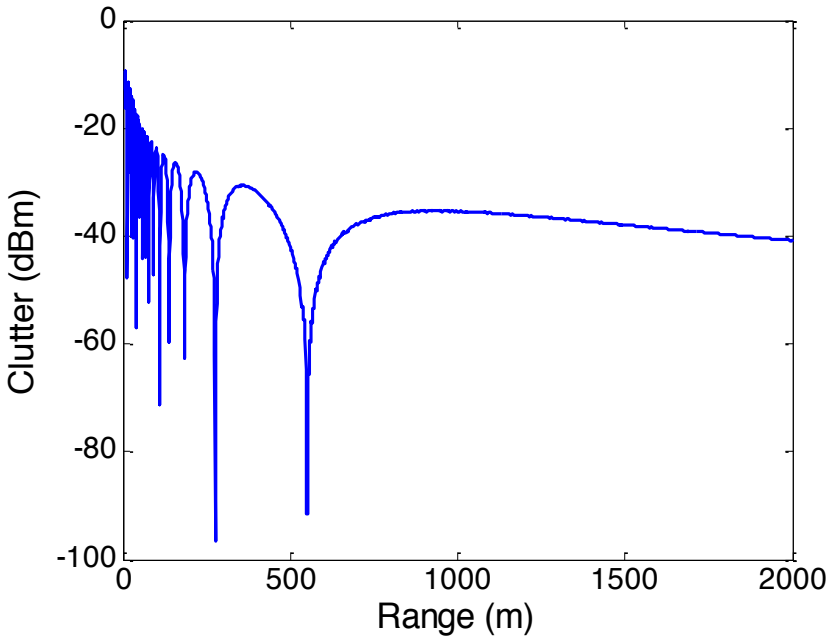

Figure 4-6. Clutter return at input to T/R module for ideal transmit pattern.

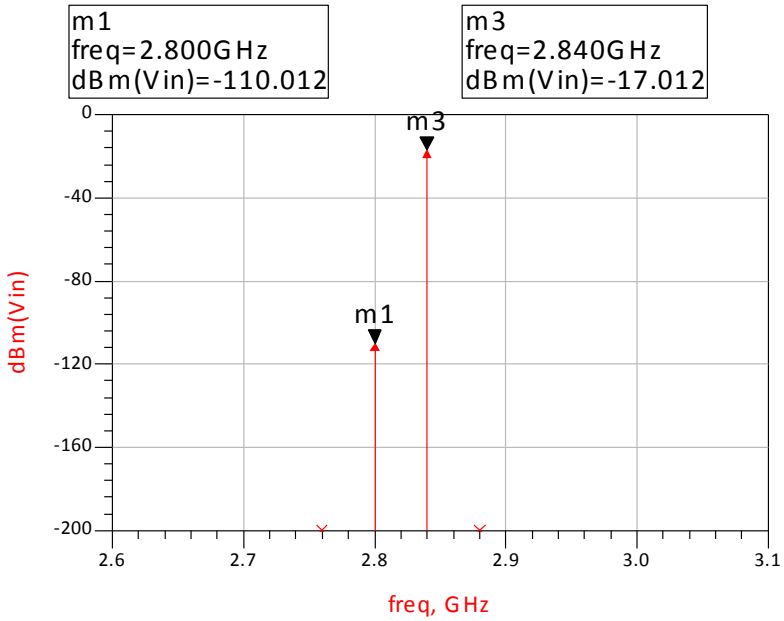

Figure 4-7. Input power of desired signal at 2.8 GHz and jamming signal at 2.84 GHz.

One might make the case for increasing the linearity of the T/R module to handle the –13 dBm clutter return. Using the standard T/R module amplitude and phase errors on the transmit beam pattern (±1 dB amplitude variation and ±10^{o} phase variation from element to element), we obtain the worst case pattern for 200 trials in Figure 4-8.

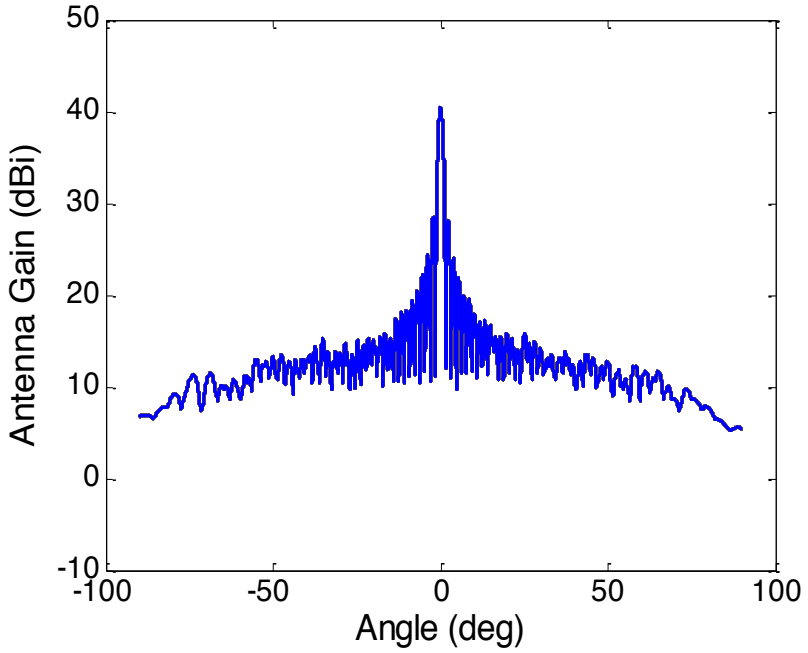

Figure 4-8. Worst case transmit pattern for 200 trials using ±1 dB amplitude and ±10^{o} phase variations from element to element.

The resulting clutter return (Figure 4-9) is higher (3 dBm) due to the higher side lobes. The linearity of the T/R module necessary to handle the power level would be significantly greater than a standard T/R module and would consume a significant amount of power since linearity and DC power are related. Thus, increasing T/R module linearity to this level is not an attractive solution.

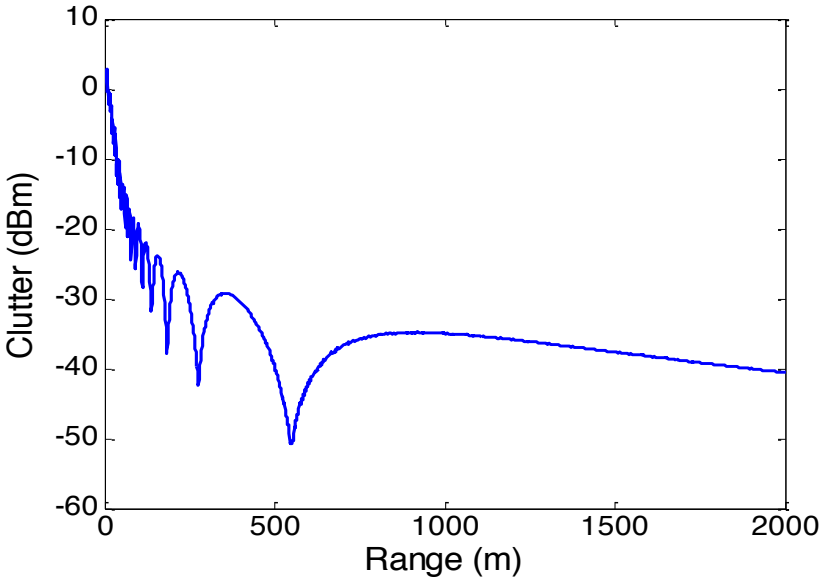

Figure 4-9. Clutter return due to degraded transmit pattern.

The clutter return with amplitude and phase errors shown in Figure 4-9 seems to imply that the use of asynchronous face operation is not possible. However, the analysis is a worst case scenario since the transmit face is pointed over into the field of view of the second receiving face at 45°. Therefore, we would like to find out over what transmit scan angles is the second face affected. Is it everywhere or only over certain scan angles? To answer this question, the transmit beam was swept from –45° to 45° and the clutter return at the second face was derived. The diagram in Figure 4-10 shows the swept transmit beam. In fact, the transmit beam could be scanned along all of the elevation angles in addition to the horizon angles. The behavior at high elevation angles may be interesting due to the transmit spoiling techniques proposed for the digital subarray architecture (Herd et al., 2010). This analysis again focused on the general problem (and in particular on the horizon scan that all phased arrays deal with) and not varying elevation scans since the particular spoiling techniques at high elevation scans are implementation specific.

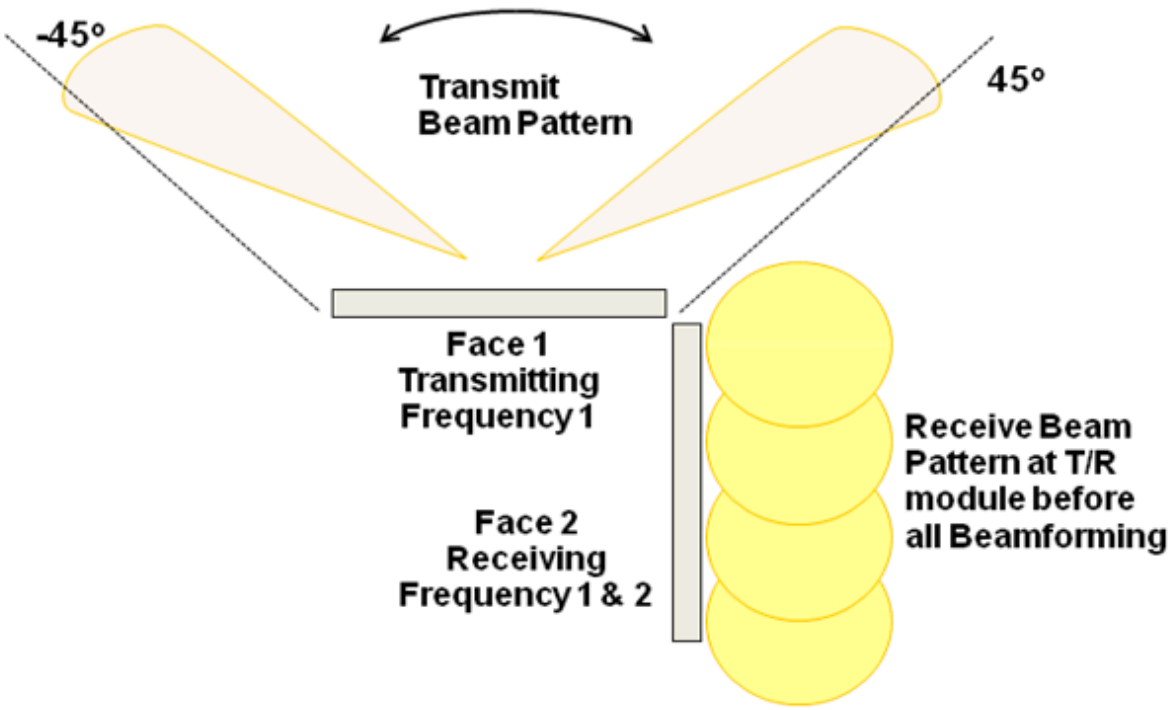

Figure 4-10. Geometry of face transmitting over –45° to 45° sector and receive antenna element with wide angular coverage.

The azimuth transmit beam pattern is calculated for each scan angle and combined with the elevation beam patterns as above. Here we will show the clutter at the range of 10 m along the ground surface. Two cases will be shown—without errors (ideal patterns in horizon and elevation planes) in Figure 4-11 and with the nominal errors (±1 dB amplitude and ±10° phase variation) in Figure 4-12. For operation with clutter less than –17 dBm, both cases (with and without errors) provide usable asynchronous operation within 1 to 3 beam positions (5°) away from scanning the transmit beam to 45°.

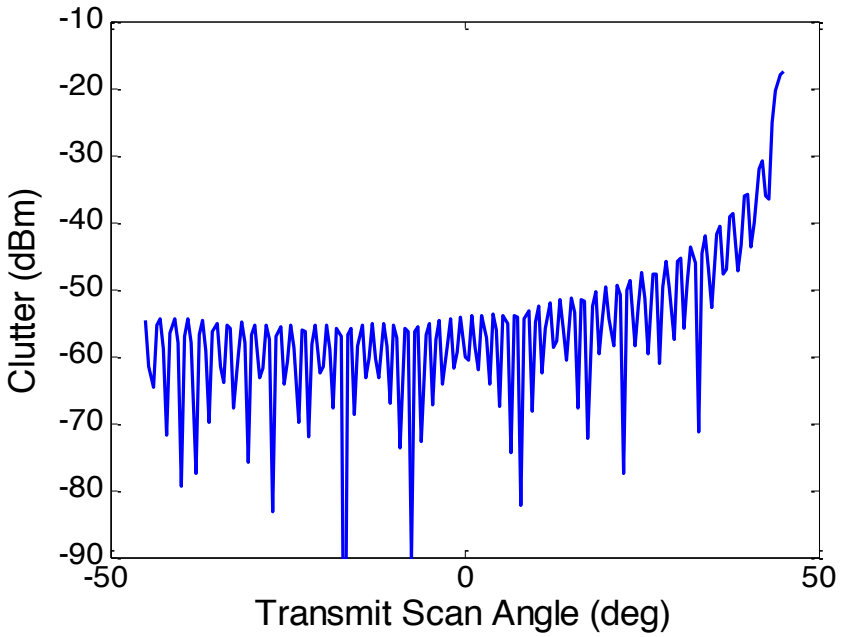

Figure 4-11. Clutter power for ideal antenna patterns at a range of 10 m along the ground.

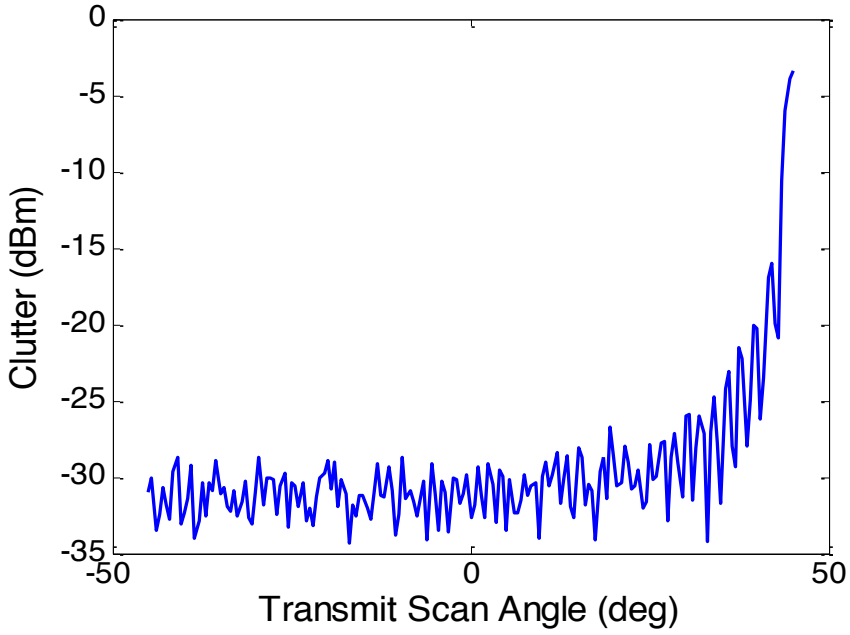

Figure 4-12. Same as Figure 4-11 except for antenna patterns with errors (±1 dB and ±10^o variation).

4.2 FULL-SIZE MPAR ANALYSIS

A similar analysis to determine the clutter returns was performed for the full-size MPAR. The assumption on tower height is that full-size MPARs are located on 30-m towers, similar to the current NEXRAD apertures. As above, we will investigate the clutter versus range for the 45° case for a transmit antenna with and without amplitude and phase errors (±1 dB and ±10°).

The full sized MPAR (8 m × 8 m) aperture has similar performance to the TMPAR (Figures 4-13 to 4-15). In general, the 45° region plus or minus several beamwidths (few degrees) is problematic but everywhere else seems feasible for asynchronous operation. The similarity in conclusion for the full-size MPAR versus the TMPAR is primarily due to the difference in tower height of 30 m vs. 15 m. The clutter equation in Figure 4-5 shows a range to the third power making increasing tower heights a significant advantage for asynchronous operation.

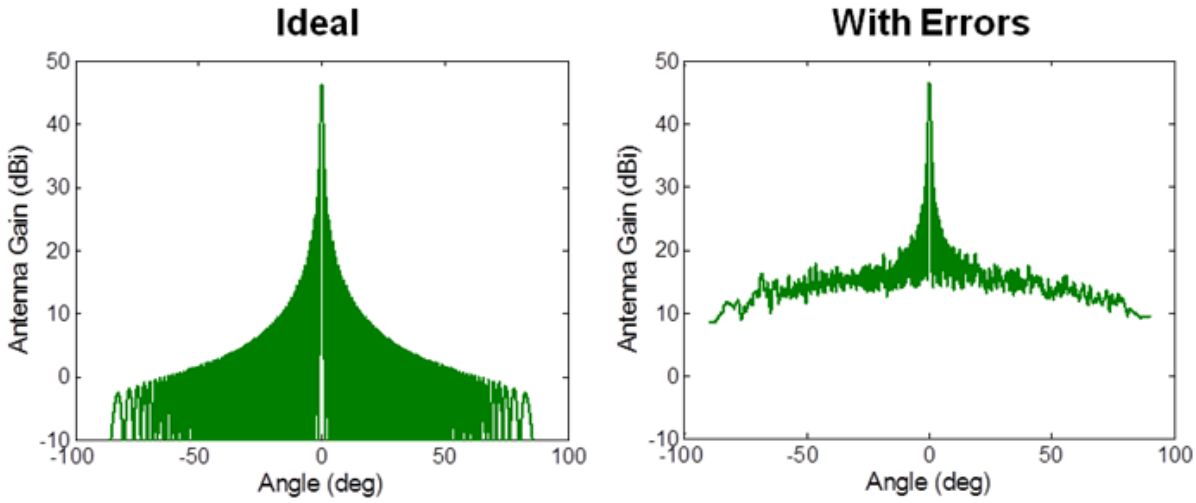

Figure 4-13. Transmit beam patterns with and without errors. (156 elements at 0.475λ spacing, corresponding to the linear dimension of an 8 m × 8 m aperture.)

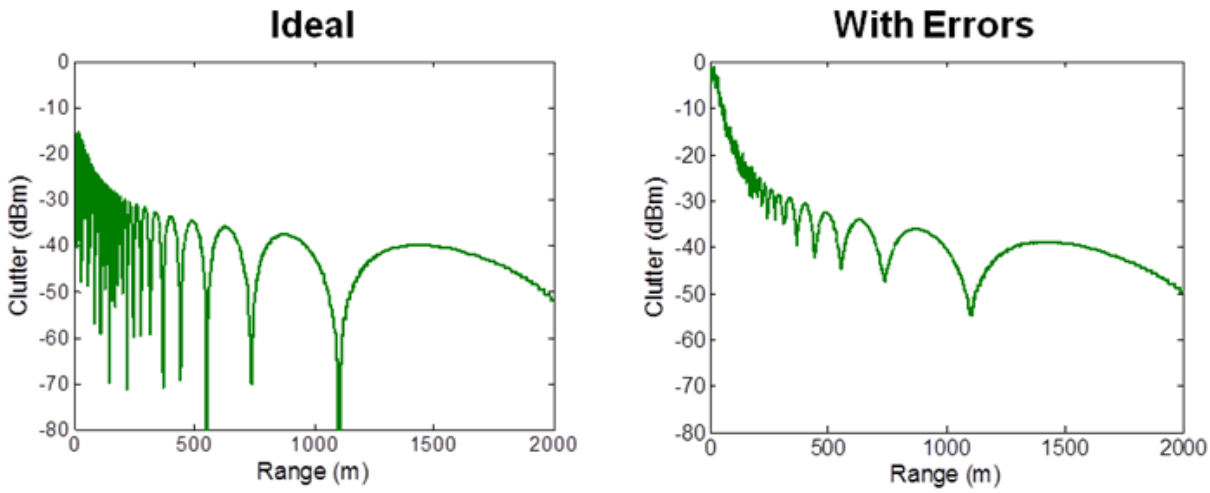

Figure 4-14. Clutter return versus range for transmit beam pointed at 45^o with and without errors.

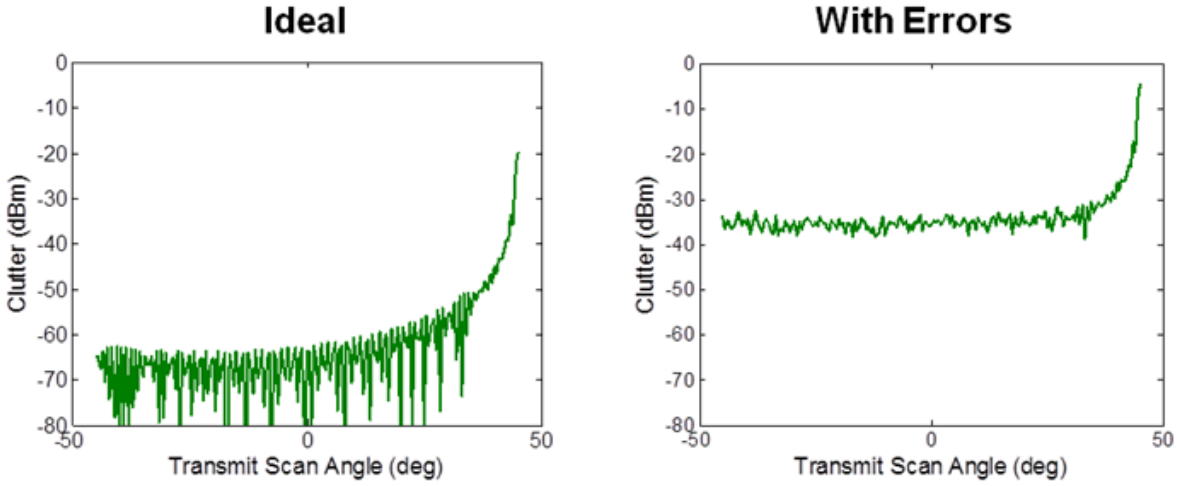

Figure 4-15. Clutter for varying transmit scan angle with and without errors.

In summary, it is a challenging problem to operate asynchronously without at least some dead gates, primarily around 45^{o} as found above. As illustrated in Figures 4-12 and 4-15 it should be remembered that the transmit beam is pointed at the 45^{o} point only ~2% of the time. A number of further mitigation strategies can be pursued including elevation pattern shaping to eliminate the side lobes pointing straight down at the ground (or at a building housing data communication equipment and other radar-associated systems as shown in Figure 4-4).

A more detailed study would be worthwhile to better understand the limits of this simplified analysis. A combination of a more detailed electromagnetic model that better included the phased array antenna with mutual coupling, radome, and building corners would be needed. In addition, some simple measurements could be constructed to better understand the tower and building implications. Although the final capability will be defined by the MPAR antenna performance, some more bounds may be understood without first building two whole apertures.

This page intentionally left blank.

5. CONCLUSION

The work described in this report addressed the following two questions. First, if spectral occupancy per radar is, indeed, increased relative to the legacy radars, will the radars be able to operate without undue interference within the allocated band? Second, could self-interference limit the ability of the MPAR to fully exploit the spectral frequency space for accomplishing its missions?

To study the first question, we estimated the single-radar spectral usage for the following operational cases: (A) All antenna faces operating at the same frequencies, (B) the front and back faces operating at the same frequencies, and (C) all faces operating on different frequencies. We also allowed each antenna face to have up to three parallel operational frequencies. The geographic locations of the MPARs and TMPARs were taken from a siting analysis detailed in a separate report. Three legacy radar replacement scenarios were examined: (1) Only the terminal aircraft and weather radars are replaced, (2) in addition to the Scenario 1 radars, NEXRADs are replaced, and (3) in addition to the Scenario 2 radars, en route aircraft surveillance radars are replaced. For all operational cases and replacement scenarios, co-channel interference between radar pairs were computed based on the single-radar results and a terrain-dependent RF propagation model. The analysis showed that there would be sufficient space in the targeted spectral window (2.7–2.9 GHz for Scenario 1, 2.7–3.0 GHz for Scenarios 2 and 3) for all cases considered. There is a caveat, however, in that the transition period when both the legacy and the new radars are operating at the same time was not studied. (Also, tactical military air surveillance radars were not included.) Therefore, a more detailed site-by-site spectral allocation analysis should eventually be conducted in conjunction with an MPAR deployment plan that specifies the exact locations of the new (or temporary) radars during the transition period.

To analyze the second question, we employed a simple bistatic ground clutter model to characterize the interference between adjacent antenna faces. (Too much interference between faces would disallow independent, asynchronous operation of the four antennas, which, in turn, would severely restrict adaptive operation that is a key attractive element of MPAR. In other words, operation would be restricted to Case A above.) The results showed that some interference is unavoidable, but it would likely only occur during times when a transmit beam was at its maximum off-broadside angle (~2% of the time). The consequent degradation in data quality due to “dead” gates in the adjacent-face receiver could be compensated for by adaptively increasing the dwell on receive. A caveat of this part of our study is that important effects such as diffraction from the radome and face edge, tower structure, and mutual coupling were not included. We recommend a follow-on study that employs a more detailed electromagnetic model that exposes the risks in fuller measure, which could also be used to explore other mitigation strategies.

This page intentionally left blank.

APPENDIX A
TABLE OF RELEVANT LEGACY OBSERVATIONAL REQUIREMENTS

Parameter	NEXRAD	TDWR	ASR-9	ARSR-4
Polarization mode	Linear H and V	Linear H	Linear V or circular	Linear V or circular
Range resolution	250 m	150 m	230 m	230 m
System dynamic range	93 dB	100 dB (instantaneous) + 26 dB STC	63 dB (instantaneous) + 60 dB STC	80 dB (after pulse compression)
First side lobe level (one-way)	–27 dB	–27 dB	–28 dB	–35 dB
Side lobe level beyond 10° (one-way)	–40 dB	–27 to –34 dB (linear decrease between 1 and 5 deg); average <–40 dB (>5 deg)	–36 dB	<–35 dB

This page intentionally left blank.

GLOSSARY

ARSR	Air Route Surveillance Radar
ASR	Airport Surveillance Radar
DC	direct current
DTED	Digital Terrain Elevation Data
FAA	Federal Aviation Administration
FM	frequency modulation
FPS	Fixed Position System
INR	interference signal to noise ratio
ISL	integrated side lobe level
MPAR	Multifunction Phased Array Radar
NEXRAD	Next Generation Weather Radar
NEXTGEN	Next Generation Air Transportation System
NOAA	National Oceanic and Atmospheric Administration
NSWRC	NextGen Surveillance Weather Radar Capability
NTIA	National Telecommunications and Information Administration
OIP3	3rd order output intercept point

PFA	probability of false alarm
POD	probability of detection
RF	radio frequency
RSEC	Radar Spectrum Engineering Criteria
SNR	signal-to-noise ratio
STC	sensitivity time control
TDWR	Terminal Doppler Weather Radar
TMPAR	Terminal Multifunction Phased Array Radar
T/R	transmit/receive
U-NII	unlicensed national information infrastructure

REFERENCES

Balanis, C.A., 2005: *Antenna Theory: Analysis and Design, 3rd ed*, Wiley.

Benner, W. E., G. Torok, M. Weber, M. Emanuel, J. Stailey, J. Cho, and R. Blasewitz, 2009: Progress of multifunction phased array radar (MPAR) program. Preprints, *25th Conf. on Interactive Information and Processing Systems for Meteorology, Oceanography, and Hydrology*, Phoenix, AZ, Amer. Meteor. Soc., 8B.3.

Cho, J. Y. N., 2006: Multifunction phased array radar pulse compression limits. Project Rep. ATC-327, MIT Lincoln Laboratory, Lexington, MA, 35 pp.

Cho, J. Y. N., S. Huang, and R. Frankel, 2012: NextGen surveillance and weather radar capability (NSWRC) siting analysis. Project Rep. ATC-391, MIT Lincoln Laboratory, Lexington, MA, 124 pp.

FCC, 2003: Revision of Parts 2 and 15 of the Commission's rules to permit Unlicensed National Information Infrastructure (U-NII) devices in the 5 GHz band. FCC-03-287, Federal Communications Commission, Washington, DC, 62 pp., http://hraunfoss.fcc.gov/edocs_public/attachmatch/FCC-03-287A1.pdf.

George, J., K .V. Mishra, C. M. Nguyen, and V. Chandrasekar, 2010: Implementation of blind zone and range-velocity ambiguity mitigation for solid-state weather radar. *Proc. 2010 IEEE Radar Conf.*, Institute of Electrical and Electronic Engineers, Washington, DC, 1434–1438.

Herd, J., S. Duffy, D. Carlson, M. Weber, G. Brigham, C. Weigand, and D. Cursio, 2010: Low cost multifunction phased array radar concept. *Proc. 2010 IEEE Int. Symp. Phased Array Systems and Technology*, Institute of Electrical and Electronic Engineers, Waltham, MA, 457–460.

Hinkle, G., 1983: Background study on efficient use of the 2700–2900 MHz band. NTIA Rep. 83-117, National Telecommunications and Information Administration, U.S. Department of Commerce, Annapolis, MD, 147 pp.

Longley, A. G., and P. L. Rice, 1968: Prediction of tropospheric radio transmission loss over irregular terrain: A computer method. ESSA Tech. Rep. ERL 79-ITS 67, Institute for Telecommunication Sciences, Environmental Science Services Administration, U.S. Department of Commerce, Boulder, CO, 147 pp.

NTIA, 2011: *Manual of Regulations and Procedures for Federal Radio Frequency Management*. May 2011 revision of the 2008 edition, Office of Spectrum Management, National Telecommunications and Information Administration, U.S. Department of Commerce, Washington, DC, 920 pp, http://www.ntia.doc.gov/files/ntia/publications/manual_5_11.pdf.

Obama, B., 2010: Unleashing the wireless broadband revolution. Presidential Memorandum, June 28, 2010, Office of the Press Secretary, The White House, Washington, DC, http://www.whitehouse.gov/the-press-office/presidential-memorandum-unleashing-wireless-broadband-revolution.

O'Hora, F., and J. Bech, 2007: Improving weather radar observations using pulse-compression techniques. *Meteorological Applications*, **14**, 389–401.

Raytheon, 1999: Digital Airport Surveillance Radar (DASR), System specification and SRD cross reference. Rev-D, CDRL No. A002-005, Contract No. F19628-96-D-0038, Raytheon Electronic Systems, Marlborough, MA, 110 pp.

Rice, P. L., A. G. Longley, K. A. Norton, and A. P. Barsis, 1967: Transmission loss predictions for tropospheric communication circuits. NBS Tech. Note 101, Institute for Telecommunication Sciences and Aeronomy, Environmental Science Services Administration, U.S. Department of Commerce, Boulder, CO, 409 pp.

Sanders, F. H., R. L. Sole, B. L. Bedford, D. Franc, and T. Pawlowitz, 2006: Effects of RF interference on radar receivers. NTIA Rep. TR-06-444, Institute for Telecommunication Sciences, National Telecommunications and Information Administration, U.S. Department of Commerce, Boulder, CO, 162 pp.

Skolnik, M., 2008: *Radar Handbook,* 3rd Ed. McGraw Hill, New York.

Ulaby, F. T., 1980: Vegetation clutter model. *IEEE Trans. Antenna Propag*., **AP-28**, 538–545.